From DEPARTMENT OF MEDICAL BIOCHEMISTRY AND BIOPHYSICS
Karolinska Institutet, Stockholm, Sweden

CALCIUM SIGNALING AND NETWORK ACTIVITY: MATHEMATICAL MODELING AND MOLECULAR MECHANISMS

Erik Smedler

Karolinska Institutet

Stockholm 2017

Cover art: light induced calcium oscillations and downstream frequency dependent phosphoprotein network.

Published by Karolinska Institutet.
Printed by AJ E-print AB

ISBN 978-91-7676-636-1

Calcium Signaling and Network Activity: Mathematical Modeling and Molecular Mechanisms

THESIS FOR DOCTORAL DEGREE (Ph.D.)

By

Erik Smedler, MSc, MD

Public defense on Monday June 12, 2017, 9.30 AM
Hillarp lecture hall, Retzius väg 8

Principal Supervisor:
Professor Per Uhlén
Karolinska Institutet
Department of Medical Biochemistry and Biophysics
Division of Molecular Neurobiology

Co-supervisor:
Professor Sten Linnarsson
Karolinska Institutet
Department of Medical Biochemistry and Biophysics
Division of Molecular Neurobiology

Opponent:
Professor Arthur Konnerth
Technische Universität München
Institute of Neuroscience

Examination Board:
Associate professor Konstantinos Meletis
Karolinska Institutet
Department of Neuroscience

Professor Anders Tengholm
Uppsala university
Department of Medical cell biology

Professor Erik Fransén
Royal Institute of Technology
School of Computer science and communication

I was looking for an equation, but found a patient

To Anna
and Henrietta Lacks

ABSTRACT

The calcium (Ca^{2+}) ion is a versatile second messenger present in all cells. It is involved in such diverse processes as cell division, differentiation, vesicle transport and muscle contraction. Its widespread applicability is partially explained by its wide temporal and spatial dynamics. By varying in time, oscillations arise and enable frequency modulation. Likewise, by varying in space, waves are formed and enable cross talk in-between cells in networks.

In here, I present novel data on the mechanism behind Ca^{2+} signaling both in the form of oscillations and in the form of intercellular networks. The investigation are performed both from a theoretical point of view using mathematical modeling simulated *in silico* and from a molecular point of view in wet-lab experiments *in vitro* and *in vivo*.

To be more specific, in **Paper I**, I present a method with software to identify functional networks in groups of cells and ways of analyzing them. In **Paper II**, this method is used to identify so-called small-world networks with scale-free properties in spontaneously active neural progenitor cells. These network formations are dependent on gap junctions and critically regulate proliferation both in neural progenitors derived from embryonic stem cells and in embryonic mouse brains.

In **Paper III**, I present a model for the generation of spontaneous Ca^{2+} oscillations in neural progenitors. The essence of this model is that the spontaneous Ca^{2+} and electrical activity is driven by functional pacemaker cells expressing slightly more voltage-gated Ca^{2+} channels than the cells connected to them with gap junctions. Interestingly, one type of channel involved in this pacemaker activity is encoded by the mental disorder susceptibility gene *Cacna1c*. Transgenic mice lacking *Cacna1c* expression in the forebrain exhibit signs of increased anxiety as well as changes in brain anatomy.

Finally in **Paper IV**, I describe a method of finding genes dependent on the frequency of Ca^{2+} oscillations. Cells stably expressing the light-sensitive protein melanopsin are exposed to light, after which the cellular content is collected and analyzed with RT-qPCR, RNA sequencing and phosphoproteomics. Hereby, a large network of genes and proteins dependent on frequency is identified.

In conclusion, the research described below deepens our understanding on Ca^{2+} oscillations and network activity, using both mathematical modeling and wet-lab molecular biology experiments.

LIST OF SCIENTIFIC PAPERS

I. **Erik Smedler***, Seth Malmersjö* and Per Uhlén
Network analysis of time-lapse microscopy recordings
Front Neural Circuits. 2014 Sep 17;8:111

II. Seth Malmersjö*, Paola Rebellato*, **Erik Smedler***, Henrike Planert, Shigeaki Kanatani, Isabel Liste, Evanthia Nanou, Hampus Sunner, Shaimaa Abdelhady, Songbai Zhang, Michael Andäng, Abdeljabbar El Manira, Gilad Silberberg, Ernest Arenas and Per Uhlén
Neural progenitors organize in small-world networks to promote cell proliferation
Proc Natl Acad Sci U S A. 2013 Apr 16;110(16):E1524-32

III. **Erik Smedler**, Roman Romanov, Débora Masini, Lauri Louhivuori, Ivar Dehnisch Ellström, Chungliang Wang, Irene Brusini, Paola Rebellato, Seth Malmersjö, Gilberto Fisone, Tibor Harkany and Per Uhlén
Spontaneous activity in neural progenitors is driven by functional pacemakers expressing the mood-disorder susceptibility gene *Cacna1c*
Manuscript

IV. **Erik Smedler**, Manuel Varas-Godoy and Per Uhlén
Genomic and proteomic analyses of impact of Ca^{2+} oscillatory frequency
Manuscript

*These authors contributed equally to the work

PUBLICATIONS NOT INCLUDED IN THIS THESIS

1) Satish Srinivas Kitambi*, **Erik S Nilsson***, Gilbert Nyah Tekeoh, Cristian Ibarra, Patrik Ernfors and Per Uhlén
Small Molecule Screening Platform for Assessment of Cardiovascular Toxicity on Adult Zebrafish Heart
BMC Physiol. 2012 Mar 26;12:3

2) Seth Malmersjö*, Paola Rebellato*, **Erik Smedler*** and Per Uhlén
Small-world networks of spontaneous Ca(2+) activity
Commun Integr Biol. 2013 Jul 1;6(4):e24788

3) **Erik Smedler** and Per Uhlén
Frequency decoding of calcium oscillations
Biochim Biophys Acta. 2014 Mar;1840(3):964-9

4) Min Wan, Oliver Söhnlein, Xiao Tang, Anne M. van der Does, **Erik Smedler**, Per Uhlén, Lennart Lindbom, Birgitta Agerberth and Jesper Z. Haeggström
Antimicrobial peptide LL-37 regulates the production of eicosanoids by human macrophages via temporally and mechanistically separate pathways
FASEB J. 2014 Aug;28(8):3456-6

5) Per Uhlén, Nicolas Fritz, **Erik Smedler**, Seth Malmersjö and Shigeaki Kanatani
Calcium Signaling in Neocortical Development
Dev Neurobiol. 2015 Apr;75(4):360-8

6) Shujie Li, Stuart M. Fell, Olga Surova, **Erik Smedler**, Karin Wallis, Zhi Xiong Chen, Ulf Hellman, John Inge Johnsen, Tommy Martinsson, Rajappa S. Kenchappa, Per Uhlén, Per Kogner and Susanne Schlisio
The 1p36 Tumor Suppressor KIF 1Bβ Is Required for Calcineurin Activation, Controlling Mitochondrial Fission and Apoptosis
Dev Cell. 2016 Jan 25;36(2):164-78

7) David Forsberg, Zachi Horn*, Evangelia Tserga*, **Erik Smedler**, Gilad Silberberg, Yuri Shvarev, Kai Kaila, Per Uhlén and Eric Herlenius
CO2-evoked release of PGE2 modulates sighs and inspiration as demonstrated in brainstem organotypic culture
eLife. 2016 Jul 5;5. pii: e14170

8) Matthias Hörtenhuber, Enrique Toledo, **Erik Smedler**, Ernest Arenas, Seth Malmersjö, Lauri Louhivuori and Per Uhlén
Mapping Genes for Calcium Signaling and Their Associated Human Genetic Disorders
Bioinformatics. 2017 Apr 19

*These authors contributed equally to the work

CONTENTS

LIST OF ABBREVIATIONS

Ca^{2+}	Calcium ion
ER	Endoplasmic Reticulum
SR	Sarcoplasmic Reticulum
$InsP_3$	Inositol triphosphate
RyR	Ryanodine receptor
GPCR	G protein coupled receptor
PLC	Phospholipase C
DAG	Diacylglycerol
CICR	Calcium induced calcium release
STIM1	Stromal interaction molecule 1
ORAI1	Calcium release-activated calcium channel protein 1
PMCA	Plasma membrane Ca^{2+} ATPase
SERCA	Sarco/endoplasmic reticulum Ca^{2+}-ATPase
VGCC	Voltage gated Ca^{2+} channel
HVA	High voltage activated
LVA	Low voltage activated
NF-κB	Nuclear Factor Kappa-light-chain-enhancer of activated B cells
MAPK	Mitogen Activated Protein Kinase
CDK	Cyclin dependent kinase
NFAT	Nuclear Factor of Activated T-cells
CaMKII	Ca^{2+}/calmodulin-dependent protein Kinase II
ERK	Extracellular related kinase
JNK	Jun amino-terminal kinase
shRNA	Short hairpin RNA
hChR2	Human Channelrhodopsin 2
eNpHR3.0	Enhanced Natronomonas pharaonis Halorhodopsin 3.0
Cx43	Connexin 43
ATP	Adenosine triphosphate
P2Y1R	P2Y purinreceptor 1
NMDA	*N*-methyl-D-aspartate
DSM	Diagnostic and Statistical Manual of Mental Disorders
SNP	Single-nucleotide polymorphism
GWAS	Genome-wide association study
LIF	Leukemia inhibitory factor

1 POPULÄRVETENSKAPLIG SAMMANFATTNING

Alla organismer inom djurriket, inklusive människan, byggs upp av celler av olika slag. Från den stund då spermien befruktar ägget börjar utvecklingen mot en vuxen människa. Denna första befruktade äggcell har kapacitet att bli vilken cell som helst i kroppen; alltifrån hjärncell till skelettcell. Denna vida utvecklingspotential härrör från att kroppens samtliga celler innehåller identiskt DNA, men att olika delar av arvsmassan är på- eller avslagen. I till exempel nerv- och muskelceller slås gener på som kodar för proteiner som har med elektrisk aktivitet att göra, medan känselceller i ögats näthinna specialiseras att bli ljuskänsliga. Vilken cell som utvecklas till vad styrs av olika signalmolekyler från övriga celler i omgivningen samt av den specifika cellens aktivitet under utvecklingen. Dessa signaler mottas sedan på cellens yta av olika specifika så kallade receptorer, vilka överför signalen till cellens insida analogt med en radioantenn. Väl inne i cellen tar sig signalen ett annat uttryck och kodas i form av olika molekyler som förändras och i sin tur förändrar andra molekyler. Det är här kalcium spelar en viktig roll i kroppens samtliga celler. Genom att förändra mängden kalcium inne i cellen på ett specifikt sätt kan signaler inkodas som en radiosignal och föras vidare till slutstationen där gener antingen slås på eller av och där redan färdiga proteiner modifieras för att bli mer eller mindre aktiva.

Detta doktorandprojekt i sin helhet har haft som mål att studera kalciumaktivitet och bildning av nätverk under hjärnans utveckling samt att utveckla metoder för att kunna styra kalciumsignaler inne i celler. I det första projektet utvecklade vi en algoritm och datorprogram för att utifrån mikroskopbilder identifiera och analysera nätverk bland populationer av celler. Denna metod användes sedan i den andra studien för att analysera de nätverk som byggs upp av spontant aktiva nervceller under utvecklingen. Vi såg här att cellerna bygger upp nätverk med likheter med exempelvis sociala nätverk och internet. Vidare fann vi att nätverken var viktiga för celldelning, så till vida att färre celler bildades när vi blockerade nätverkskopplingarna. I musembryon ledde denna blockad till att hjärnorna blev mindre.

I det tredje projektet har vi försökt förstå vad som ger upphov till spontanaktiviteten hos omogna nervceller. För detta utvecklade vi en matematisk modell som vi simulerade i en dator för att få förutsägelser att testa i experiment. Genom detta såg vi att en kalciumkanal som öppnas när spänningen över cellmembranet stiger troligtvis är viktig. Intressant nog kodas denna för av en känd riskgen för bipolär sjukdom och schizofreni. Vi utvecklade därför även en musmodell där denna gen har slagits ut i en del av hjärnan. Intressant nog har dessa möss tecken på ökad ångest och förändringar i hjärnans anatomi.

I det fjärde projektet har vi utvecklat en metod för att med blått ljus kunna styra kalciumaktiviteten inne i celler. Genom detta ville vi studera hur celler kan avkoda skillnader i frekvenser hos kalciumoscillationer, på samma sätt som en radiosignal kan frekvensmoduleras. Celler stimulerades med antingen hög (en gång varje minut) eller låg frekvens (en gång varannan minut), varefter cellernas innehåll analyserades. Genom denna analys har vi funnit en mängd olika gener och proteiner som svarar specifikt på förändringar i frekvens.

2 INTRODUCTION

2.1 CALCIUM SIGNALING

Living organisms all exploit intricate signaling pathways to activate, maintain or inhibit function, growth, differentiation and apoptosis. In the nervous system, neurons are communicating with electrical impulses, creating cellular networks that perform computations. In the developing brain, cells not only divide and migrate, but also form networks resembling the adult equivalents. During embryonic development and differentiation of stem cells, cells are constantly communicating, resulting in tissue specific gene expression. These signals are partially mediated via Ca^{2+} signaling. One has estimated there are around 20 different intracellular signal transduction modules [1]. Among these, five are related to Ca^{2+} signaling, involved in as diverse processes as fertilization, apoptosis, proliferation, differentiation, muscle contraction and learning [2-6]. The signals are created by the four orders of magnitude large concentration gradient between the cytosol and the extracellular fluid as well as in cytoplasmic compartments such as the endoplasmic reticulum (ER) [5, 7]. Ca^{2+} waves can spread to adjacent cells either via gap junctions or in a paracrine fashion [8]. The Ca^{2+} oscillations are used as a medium for transmitting signals to be decoded and taken action for in the cell. As in a radio transmitter, the signals can be both frequency and amplitude modulated [9].

2.2 CALCIUM SIGNALING TOOLKIT

Cells normally keep their intracellular Ca^{2+} concentration around 100 nM, while the extracellular concentration is approximately four orders of magnitude higher at 1 mM. Different intracellular organelles have different concentrations of Ca^{2+}, for example 100 μM in the ER. The extracellular concentration is controlled by hormones such as parathyroid hormone from the parathyroid gland that increases the concentration and calcitonin from the thyroid gland that decreases the concentration of Ca^{2+}.

Cells themselves, however, keep the homeostasis by expressing a unique set of transporters; sometimes called the Ca^{2+} signaling toolkit (see **Figure 1** for cartoon). Here, the cytosolic concentration of Ca^{2+} can increase due to influx via ion channels (voltage operated, VOC, or receptor operated, ROC) in the plasma membrane or via the inositol triphosphate ($InsP_3$) receptor or ryanodine receptor (RyR) in the ER or sarcoplasmic reticulum (SR). This is denoted by red color in the cartoon in **Figure 1**. The $InsP_3$ receptor is a membrane glycoprotein that acts a Ca^{2+} channel and is activated by $InsP_3$ [10]. $InsP_3$ is synthesized together with diacylglycerol (DAG) as phosphatidylinositol 4,5-bisphosphate is hydrolyzed in the plasma membrane by phospholipase C (PLC). PLC in turn is activated by ligands binding to G protein coupled receptors (GPCR) coupled to a G_q heterotrimeric G protein. In **Paper IV**, the G_q protein melanopsin was activated by light, leading to PLC activation and downstream Ca^{2+} increase. The open probability of both $InsP_3R$ and RyR are dependent on cytosolic Ca^{2+} and involved in so-called Ca^{2+} induced Ca^{2+} release (CICR). Studies have found a bell shaped dependency curve for Ca^{2+} [11]. Efflux of Ca^{2+} from the ER/SR leads to store depletion and activation of the sensor protein STIM1 via its EF hand domain. STIM1 activation in turn leads to activation of ORAI1 channels in the plasma membrane and thus influx of Ca^{2+} [12]. After elevation of cytoplasmic Ca^{2+}, the concentration may return to

baseline via the action of energy dependent pumps on the plasma membrane (plasma membrane Ca^{2+} ATPase, PMCA) or ER/SR membrane (sarco/endoplasmic reticulum Ca^{2+}-ATPase, SERCA). This is denoted by blue color in the cartoon in **Figure 1**. Ca^{2+} oscillations appear when this rise and fall of cytosolic Ca^{2+} happens repeatedly in time. Changes of Ca^{2+} in the space domain are called waves.

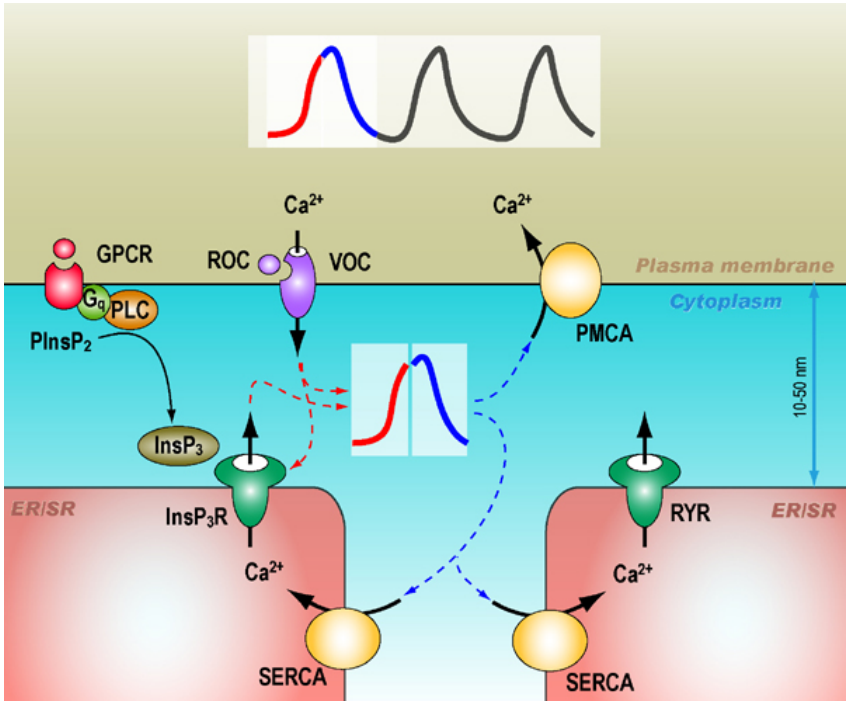

Figure 1 Calcium signaling toolkit, courtesy of Per Uhlén.

2.3 VOLTAGE GATED CALCIUM CHANNELS

Voltage gated Ca^{2+} channels (VGCC) are plasma membrane ion channels mainly selective for Ca^{2+} that are activated upon depolarization. See for example [13] for review. The channels are complex proteins with four or five subunits encoded by multiple genes. The α_1 subunit constitutes the ion-conducting pore as well harness voltage sensing, gating mechanisms and ligand binding sites. It is also used for the taxonomy. The auxiliary subunits modulate the channel complex, but have little effects on the channel properties. See **Table 1** for summary of function and localization.

Another division can be made on basis of voltage dependence. L, P/Q, N and R are high voltage activated (HVA) channels, meaning they require strong depolarization in order to be activated. T type channels on the other hand are low voltage activated channels (LVA), meaning they require weaker depolarization for activation.

Table 1 List of voltage gated calcium channels. Adapted from [13].

Channel	Current	Gene	Function	Localization
$Ca_V1.1$	L	*CACNA1S*	Excitation-contraction coupling	Skeletal muscle
$Ca_V1.2$	L	*CACNA1C*	Excitation-contraction coupling, hormone release, transcription and synaptic integration	Cardiac muscle, smooth muscle, endocrine cells and neurons
$Ca_V1.3$	L	*CACNA1D*	Hormone release, transcription, synaptic regulation, cardiac pacemaking, hearing and neurotransmitter release from sensory neurons	Endocrine cells, neurons, cardiac muscle and cochlear cells
$Ca_V1.4$	L	*CACNA1F*	Neurotransmitter release from photoreceptors	Retina, spinal cord, adrenal gland and mast cells
$Ca_V2.1$	P/Q	*CACNA1A*	Neurotransmitter release, dendritic firing and hormone release	Neurons and neuroendocrine cells
$Ca_V2.2$	N	*CACNA1B*	Neurotransmitter release, dendritic firing and hormone release	Neurons and neuroendocrine cells
$Ca_V2.3$	R	*CACNA1E*	Repetitive firing, dendritic firing	Neurons
$Ca_V3.1$	T	*CACNA1G*	Pacemaking, repetitive firing	Neurons, cardiac muscle and smooth muscle
$Ca_V3.2$	T	*CACNA1H*	Pacemaking, repetitive firing	Neurons, cardiac muscle and smooth muscle
$Ca_V3.3$	T	*CACNA1I*	Pacemaking, repetitive firing	Neurons

2.4 CALCIUM AND PROLIFERATION

Cell division is the final output of an active cell cycle and is controlled by a complex network of phosphorylations and dephosphorylations. Cyclin dependent kinases (Cdk) are activated upon mitogenic signals when bond to their corresponding cyclins. Ca^{2+} is known to be involved in different aspects of cell cycle control, for instance in G1-S transition [14]. For example in embryonic stem cells, $InsP_3$ mediated Ca^{2+} oscillations are mostly confined to the

G1-S transition [15]. In starved fibroblasts, serum induced Ca^{2+} activity was necessary for cell cycle progression via cyclin D1 and the MAPK-NF-κB (Nuclear Factor kappa-light-chain-enhancer of activated B cells and Mitogen Activated Protein Kinase) pathway [16].

2.5 ENCODING AND DECODING

The transformation of a biological signal from for example ligand-receptor interaction to intracellular signal transduction with Ca^{2+} is here called encoding and is reversed by decoding, where different types of molecules sense the dynamics and change their activity accordingly. This process is equivalent to electromagnetic radiation being received by an antenna and translated to sound in a radio. Mathematical modeling of a generic Ca^{2+} sensitive protein has shown the possibility of Ca^{2+} oscillations to be decoded on basis of the frequency itself, the duration of the single transients or the amplitude [17]. In summary, oscillation frequency is correlated with target activity. The molecular mechanism behind the decoding is thought to include on-and-off kinetics of Ca^{2+} binding to kinases and phosphatases, activating and inactivating target proteins respectively. If the frequency of oscillations is much lower than the typical on/off frequency, no integration will occur and the signal is simply decoded as a sum of single transients. Oscillations are more effective in activating the target than a constant signal when Ca^{2+} is bound cooperatively and with low affinity. The list of frequency decoding proteins has been constant for a while and include: NF-κB, MAPK, NFAT (Nuclear Factor of Activated T-cells), CaMKII (Ca^{2+}/calmodulin-dependent protein Kinase II) and calpain. See **Figure 2** and our review for more information [18].

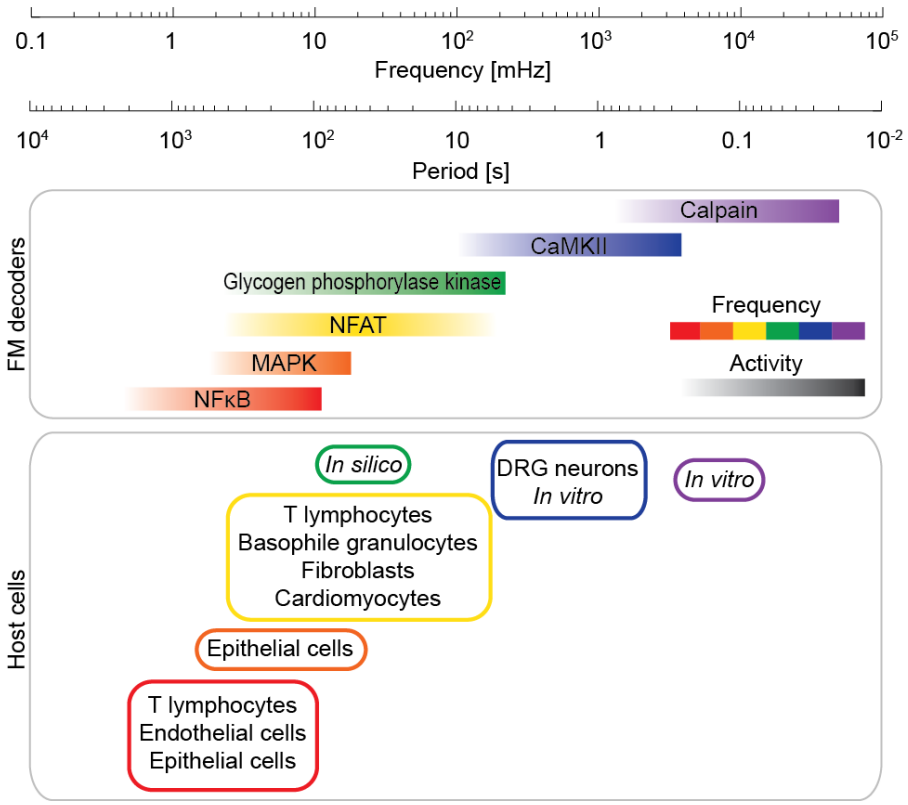

Figure 2 Overview of frequency dependent proteins.

In the canonical pathway, both NF-κB and NFAT are dependent on dephosphorylation by calcineurin, followed by translocation to the nucleus where they modulate transcription. The Ca^{2+} binding protein calmodulin in turn activates calcineurin by phosphorylation. The so-called integrative tracking model, were NFAT and NF-κB are sequentially phosphorylated and de-phosphorylated, is thought to explain the frequency dependence [19]. The MAPK family consists of three groups: p38 MAPKs, extracellular signal-related kinases 1 and 2 (ERK1/2) and Jun amino-terminal kinases (JNKs). The ERK pathway has been shown to be frequency decoding by being activated by upstream Ras guanine nucleotide exchange factors [20]. On the other hand, CaMKII is activated by auto-phosphorylation after binding to calmodulin and Ca^{2+} [21]. Clearly, there are fundamentally different mechanisms behind frequency decoding, which is reflected by different dynamics. NFAT and NF-κB have so far been reported to be frequency decoders in the low frequency range around 1-10 mHz, whereas CaMKII decodes around 100-1000 mHz [18]. In **Paper IV**, cells are exposed to Ca^{2+} oscillations in the range 10-50 mHz.

2.6 CONTROLLING CALCIUM IN EXPERIMENTS

Almost all studies on Ca^{2+} oscillations and molecular decoding are observational or crudely interventional. Researchers observe spontaneous and ligand-induced activity and thereafter try to block the activity by applying different drugs or shRNAs. One established, but rarely used method is the so called Ca^{2+} clamp that is both non-physiologic and possesses low temporal and spatial controllability [22]. See **Figure 3A** for an example. Recent technological breakthroughs in optics and genetics (optogenetics) provide us with tools to manipulate and control Ca^{2+} signaling in living cells. Optogenetics takes advantage of (not exclusively) two ion transporters, channelrhodopsin-2 (hChR2) [23] a light-activated cation channel, and halorhodopsin (eNpHR3.0), a light-driven ion pump [24] as well as the G-protein coupled receptor melanopsin [25]. Heterologous expression of these transporters into cells that are stimulated with light at certain wavelengths changes the membrane potential and activates or inactivates voltage gated Ca^{2+} channels (ChR2 and NpHR) or activates phospholipase C (PLC) leading to Ca^{2+} influx from the ER. See **Figure 3B** for an example with light controlled oscillations using melanopsin.

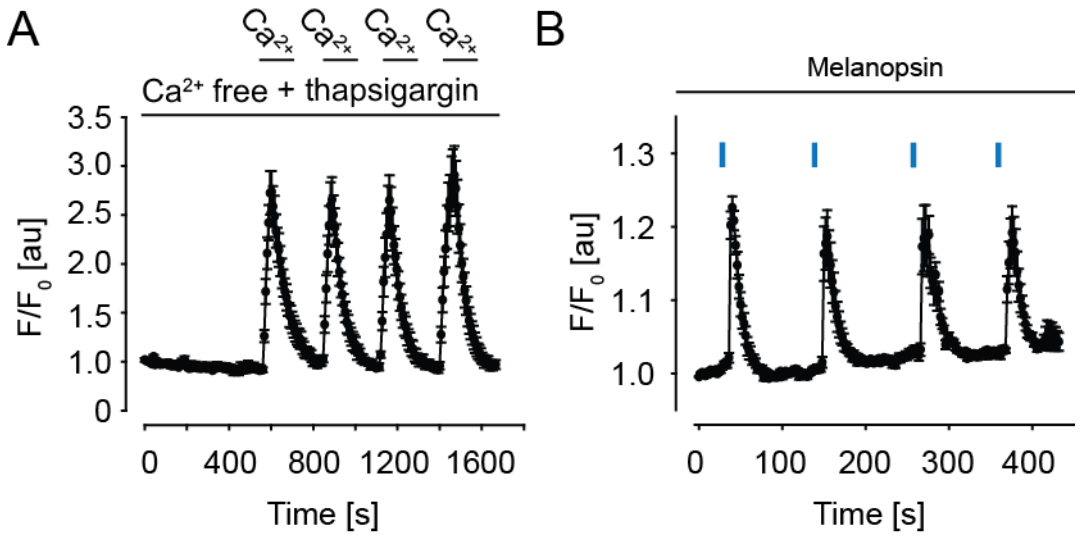

Figure 3 A) Calcium clamping using thapsigargin. B) Light controlled oscillations using melanopsin.

2.7 NETWORKS

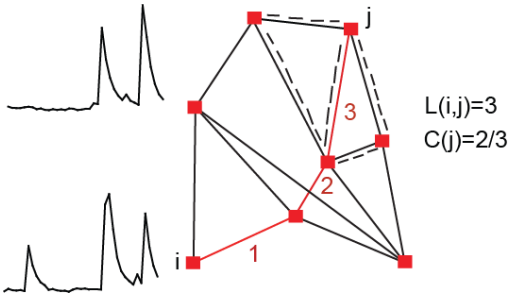

Figure 4 Network based on correlated Ca^{2+} activity.

The notion of graphs (mathematical term for networks) was established already in 1736 by the Swiss mathematician Leonard Euler, analyzing the possibility of different paths in a network consisting of islands and bridges. A graph formally consists of a set of vertices (nodes) and edges (links), connecting the nodes [26]. See **Figure 4** for an example with nodes as red squares and links as black lines. Nodes might be of different sizes, ranging from single proteins to single cells and cortical areas. The links on the other hand range from physical protein-protein interactions [27] and intercellular ion fluxes [28] to axon bundles [29]. Intriguingly, empirical networks are neither random nor regular, but appear to follow certain structural rules (so called small-world and scale-free networks) [30, 31]. For instance in social networks and in internet the mean internodal topological distance is much shorter than expected, clustering is higher and highly connected nodes (hubs) exist with a non-zero probability. The shortest path-length is the minimum number of nodes that must be passed in order to travel from one node to another (see red straight line in **Figure 4**. The clustering coefficient is the number of neighbors of a node that are also neighbors of each other divided by the total number of possible links between the neighbors (see the neighbors of j in **Figure 4**).

2.8 GAP JUNCTIONS

Gap junctions are direct intercellular connection in-between the cytoplasm of neighboring cells (**Figure 5**). The channels are composed of two hemi channels called connexons. The connexons themselves are in vertebrates usually homo- or heterohexamers of connexins. In humans, 21 different connexin genes are expressed [32]. One of the mostly studied connexins is connexin43 (Cx43), with a molecular weight of 43 kDa. Cx43 is ubiquitously expressed and is vital in for example electrical signaling in cardiac muscle cells and neural development [33].

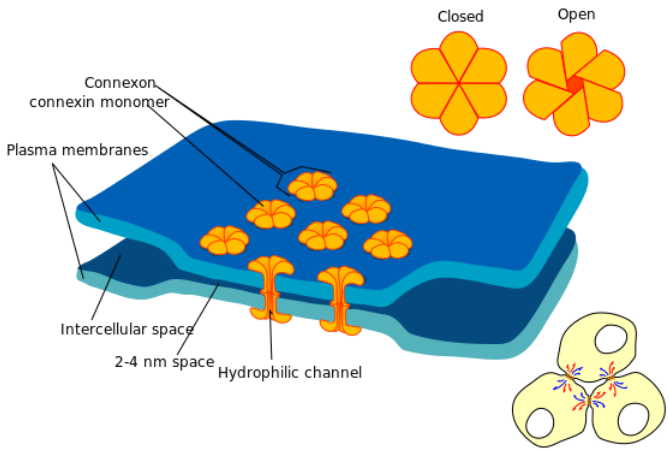

Figure 5 Cartoon of gap junction connection. Courtesy of Mariana Ruiz, Wikipedia.

Gap junctions enable transport of electrical current as well as molecules smaller than approximately 500 Da [34]. Gap junctions are highly expressed during embryonic development and may provide a structure for intercellular communication before mature synaptic networks are formed [35]. Interestingly, there is a switch from expression of mainly Cx26 and Cx43 in the embryonic cerebral cortex to mainly Cx32 postnatal.

2.9 NEURAL DEVELOPMENT

The zygote is formed as the sperm fertilizes the oocyte. Without any significant growth, the zygote divides and forms a blastocyst in mammals (**Figure 6)**. The cells of the inner cell mass of the blastocyst are pluripotent (often called embryonic stem cells) and may differentiate to any kind of cells in the developing organism. After seven days in humans, the blastocyst is implanted in the uterus for further development and gastrulation. After twelve days, a bilaminar disc is created and is the basis for the future ectoderm and endoderm. Next, a three-layered gastrula is formed and the embryo changes its topology from a simply connected sphere like structure to a non-simply connected torus like structure.

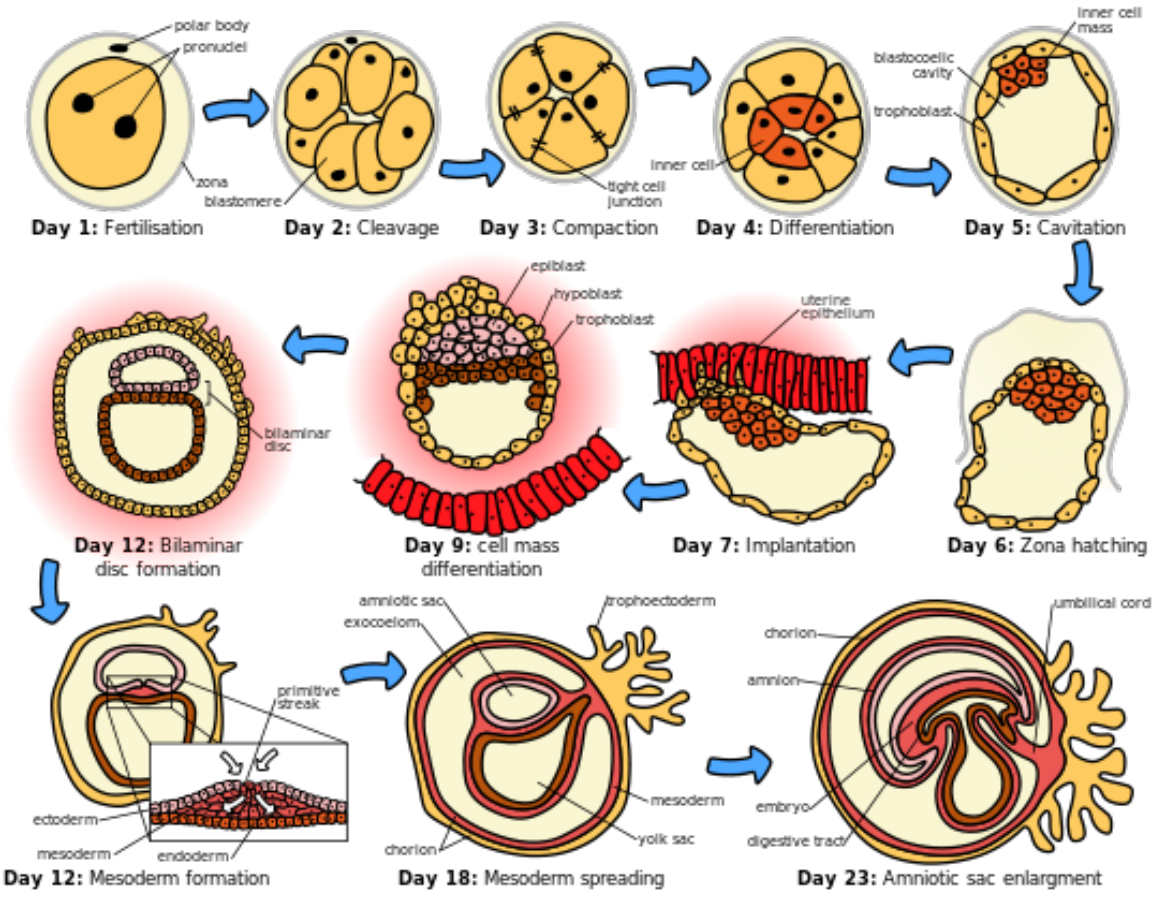

Figure 6 Early embryogenesis in humans. Wikipedia.

Neurulation follows gastrulation as the thickened plate called the neural plate is formed by the ectoderm. Upon folding, the plate is converted to a tube (around week four in human embryogenesis). Next, the tube is expanded radially, differentially along the anterior-posterior axis. As a glass blower makes beautiful art out of sand, this expansion is the

prototype of the future brain with its different components. The walls of the neural tube are constituted by neuroepithelial cells, which are the grandparents of all cells in the mature nervous system. The neural tube forms four different structure that later on will develop to separate regions in the central nervous system: the prosencephalon (forebrain), the mesencephalon (midbrain), the rhombencephalon (hindbrain) and the spinal chord (see **Figure 7**) in rostral to caudal direction. The prosencephalon will later develop into the telencephalon and diencephalon. The dorsal telencephalon, also called pallium, will form the cerebral cortex, whereas the ventral telencephalon, subpallium, will form the basal ganglia. The diencephalon will later form the thalamus, hypothalamus, epithalamus and subthalamus. Finally, the cerebral cortex will among other things form the neocortex and hippocampus.

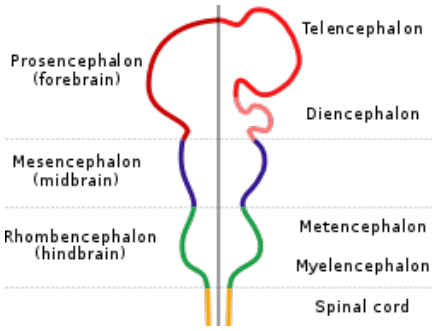

Figure 7 The main subdivisions of the embryonic vertebrate brain**.** Wikipedia.

The formation of different regions during neural development is controlled by genetic programs that in turn are governed by different transcription factors. In the spinal cord and hindbrain, *Hox* genes provide segmental information [36]. The rostral central nervous system on the other hand is regulated by its own factors, for instance *Emx1*, *Emx2*, *Otx1* and *Otx2* in mice [37]. *Emx1* is expressed exclusively in the dorsal telencephalon, irrespective of whether cells are proliferating, differentiating or migrating and can be seen already around E10 in mouse embryos [38]. In **Paper III**, *Cacna1c* was deleted in Emx1 positive cells.

Spontaneous Ca^{2+} activity is a hallmark of neural development and is thought to run in parallel to and interact with the genetic programs [4, 39]. Spontaneous activity has been found and characterized in neuronal synaptic networks in the retina [40], spinal cord [41], auditory nerve [42], hippocampus [43] and cerebellum [44]. One may speculate that embryonic network activity may shape the structure of the mature network, including downstream effects. For instance in the retina of newborn ferrets, wave like spontaneous electrical activity was seen, possibly affecting neural circuitry in the lateral geniculate [40]. Many different mechanisms for the generation of activity have been proposed in different systems, including depolarizing action of GABA (as opposed to the traditional inhibitory effect due to differential expression of chloride transporters [45]) and formation of transient synaptic connections and the presence of pacemaker-like neurons [46].

However, non-synaptic activity is also important, especially earlier during development. Several studies have reported spontaneous activity in the embryonic and early postnatal cerebral cortex of mice [47, 48] and rats [8, 49, 50]. In intermediate neural progenitor cells in E16 mice, migration from the ventricular zone to the subventricular zone is dependent on ATP based Ca^{2+} signaling via the P2Y1 receptor [48]. During the same developmental stage, spontaneous Ca^{2+} oscillations control interkinetic translocation of ventricular zone neural progenitors [47]. The activity is dependent on ATP release through gap junction hemichannels, intercellular diffusion of Ca^{2+} through gap junctions and subsequent activation of $InsP_3R$. Measuring proliferation in the ventricular zone of rat embryos, another team found

spontaneous waves of Ca^{2+} to be essential [51]. Once again, this activity was shown to be dependent on gap junction hemichannels, P2Y1 receptors and intracellular Ca^{2+} release.

2.10 MATHEMATICAL MODELING

In the exact sciences, mathematical modeling is essential. Experimental results are tested against predictions from previous mathematical models. The models themselves are supposed to be as simple as possible and derivable from past principles. However, as the systems studied become more complex, the models that describe them in mathematical terms become so complex that exact solutions are impossible. For instance, it is only for the hydrogen atom that the so-called Schrödinger equation can be solved analytically, and the different energy levels of the electrons can be calculated exactly. For all other atoms, simulations are needed. It is a truism to say that biology is the study of living matter that is far more complex and complicated than the atoms that are the building stones. Still, mathematical modeling can be a useful also in biomedicine. It is all a matter of the level of abstraction, where for instance individual units in a network of multiple cells can be modeled as zero-dimensional points if only the dynamics in time is of interest.

2.11 MENTAL DISORDERS

In modern clinical medicine, neurological diseases are diagnosed and treated by neurologists, whereas psychiatrists handle mental disorders. Traditionally, mental disorders are characterized by change in function of the nervous system but with no clear organic correlate. However, as the origin of the mind is the central nervous system, it is a truism to say that every mental disorder must have an organic correlate. A striking, but rare, example of this is the so-called anti-NMDA receptor encephalitis [52]. In this immunological disease, patients present with psychosis and agitation and are admitted to psychiatric units. As the disease progresses, the patients may develop autonomic dysfunction, ataxia and paresis. The etiology is now known to be autoantibodies against one of the subunits of the NMDA receptor, developed especially as a paraneoplastic phenomenon in young females with ovarian teratomas.

Figure 8 Self-portrait of a person with schizophrenia. Courtesy of Craig Finn.

Bipolar disorder is a serious mental disorder characterized by periods of elevated mood (mania or hypomania) as well as periods of depression [53]. Depending on the severity, patients may experience psychosis. The lifetime prevalence of bipolar disorder is around one percent and primarily affects young adults with a life-long disability [54]. There is no curative treatment, although mood stabilizers such as lithium and anticonvulsants may be used. The pathogenesis of bipolar disorder is unknown, but there is a strong genetic component. The overall heritability has been estimated at 0.71 [55]. Schizophrenia may be considered an even more debilitating psychiatric disease also affecting young adults and with a life-long disability. The global lifetime prevalence is around 0.4 percent

[56]. Schizophrenic patients have both positive symptoms, such as delusions and hallucinations, and negative symptoms, such as anhedonia and emotional blunting. See **Figure 8** for self-portrait by a patient. Classical antipsychotic drugs primarily target the dopamine system with rather high efficacy on positive symptoms, but low on the negative symptoms. The overall heritability is estimated at 0.9 [57].

Traditionally, bipolar disorder and schizophrenia are considered to be completely separated and belong to different groups of diagnoses in for example the Diagnostic and Statistical Manual of Mental Disorders (DSM-5). However, apart from sharing many features of symptomatology, there is a strong genetic coupling between schizophrenia and bipolar disorder [58]. Several interesting single-nucleotide polymorphisms (SNP) have been detected at a genome-wide significance level in genome-wide association studies (GWAS) [59, 60]. Among a few other genes, *CACNA1C* was considered an interesting risk gene [61]. *CACNA1C* encodes the alpha 1c subunit of the L-type voltage gated calcium channel $Ca_V1.2$, increasing the cytosolic Ca^{2+} concentration upon strong depolarization [62, 63]. The channels are thought to play an important role in for example excitation-transcription coupling, neuronal survival and synaptic efficacy [64-66].

3 AIMS

The overall aim of this thesis was to investigate the temporal and spatial dynamics of Ca^{2+} signaling in eukaryotic cells, especially in the nervous system. In specific, the aims were:

AIM 1

To develop a method to identify and analyze functional networks in cells.

AIM 2

To investigate spontaneous Ca^{2+} activity in neural progenitors and the functional networks that are dependent on it.

AIM 3

To investigate the role of the mood disorder susceptibility gene *Cacna1c* in spontaneous Ca^{2+} oscillations.

AIM 4

To investigate frequency modulation of Ca^{2+} oscillations.

4 METHODOLOGY

4.1 CELL CULTURE

In **Papers I-IV**, several different kinds of cells have been cultured and employed in experiments: HeLa (human cervical carcinoma cells), SH-SY5Y (human neuroblastoma cells), HL-1 (mouse atrial cardiomyocyte tumor cells) and R1 mES (mouse embryonic stem cells). Standard cell culture methodology was employed. The embryonic stem cells were used as an *in vitro* model of differentiation. Cells were kept undifferentiated in certain proliferation media with leukemia inhibitory factor (LIF) in gelatin coated plastic dishes. Neural differentiation was induced by seeding cells at certain density (around 100 000 cells in a 35 mm petri dish) with media without LIF but supplemented with N2 and B27 [67]. An initial phase of massive apoptosis was followed by gradual differentiation, which visually could be seen as growth of extensions.

4.2 ANIMAL MODELS

Mice were used as model systems in **Papers II-III**. All experiments were approved by Stockholm's Ethical Committee North (ethical approval no. 256/10, no. 40/15 and no. 47/13). In **Paper III**, knockout mice were established using Cre-Lox recombination. Starting from mice purchased from the Jackson Laboratory (*STOCK Cacna1ctm3Hfm/J* and B6.129S2-Emx1tm1(cre)Krj/J), experimental mice were established: *LoxP-Cacna1c*$^{+/+}$*:Cre-Emx1*$^{+/-}$ (knockout) and *LoxP-Cacna1c*$^{+/+}$ *:: Cre-Emx1*$^{-/-}$ (control). In this system, exons 14 and 15 of the *Cacna1c* gene are flanked by loxP sites in all cells. Cre, on the other hand, is expressed in Emx1 positive cells exclusively (mainly in the forebrain). In these cells, loxP sites are recognized by Cre recombinase.

4.3 STATISTICAL CONSIDERATIONS

No power analyses were performed prior to experiments in order to estimate sample sizes for experiments. In general, at least three biological replicates were used and hypothesis testing for sample means was performed using Student's t test.

In **Paper I**, statistical significance of functional network links was estimated employing a bootstrapping method. For the entire data set, time-traces were randomly shuffled and correlation values calculated. As cutoff for significance, the 99th percentile of shuffled data was used. In **Paper IV**, hypothesis testing for RNA sequencing and phosphoproteomics data was done using Student's t test. Differentially expressed genes and differentially phosphorylated proteins were selected by both p value (adjusted for multiple comparisons) and fold change. Data to analyze is discrete, reflecting the counting of sequenced molecules. Normalization, however, leads to data being rather continuous. There is a vast literature on how to statistically model RNA sequencing data [68]. In some approaches, counts are modeled with the Poisson or negative binomial distribution.

Handling multidimensional data raises the issue with multiple comparisons. Performing m separate hypothesis tests at significance level α leads to on average $m\alpha$ false positives. For instance, comparing 20 000 genes with significance level 0.05 would lead to 1000 false positive genes. The classical, but largely underpowered, method to control for this is by performing the so-called Bonferroni correction by dividing the threshold with the number of independent hypothesis tests:

$$\propto_{Bonferroni} = \frac{\propto}{m}$$

A more powerful method is to calculate the false discovery rate (FDR), in which one only takes into account the number of false positives in the subpopulation of rejected hypotheses. One may estimate the FDR by considering the shape of the distribution of p values, as firstly described by Benjamini and Hochberg [69]. The underlying assumption is that the null hypothesis has a uniform p value distribution, whereas the alternative distribution has a peak closer to 0 (see **Figure 9A**). The q values are defined as the minimum FDR attained at or above a given score and are analogous to p values, but in terms of FDR and not false positive rate. See **Figure 9B** for relation between p values and q values.

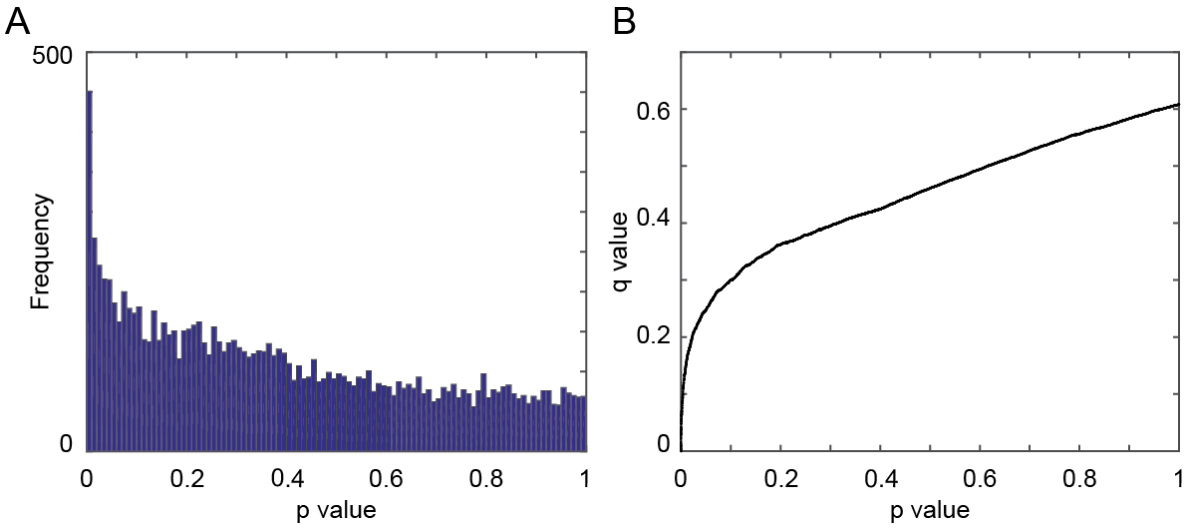

Figure 9 A) Distribution of p values for RNA sequencing data B) q values as a function of p values.

4.4 CALCIUM IMAGING

The Ca^{2+}concentration in this thesis was measured in living cells using fluorescent dyes and time-lapse microscopy. In general terms, Ca^{2+} fluorophores are molecules that can bind to Ca^{2+} with a certain affinity and change its fluorescence intensity. The first widely used dye was Fura-2 [70], which is a so-called ratiometric dye enabling absolute measurements after calibration (of essential use in [71]). Two different ultra-violet wavelengths are used to excite Fura-2, and one wavelength of green light is emitted. One of the wavelengths increases in intensity as Ca^{2+} decreases, whereas the other increases as Ca^{2+} increases. Taking the ratio results in an absolute value. Other dyes, such as Fluo-3/4/8 are non-ratiometric and do not enable calibration in the same sense. However, often the absolute level of Ca^{2+} is of low interest. For example, when measuring spontaneous activity in neurons, the dynamics in time

is not heavily dependent on the exact concentration of Ca^{2+}. Different dyes have different spectra and kinetics, enabling a great variety of experimental setups and combinations. In **Paper IV**, Ca^{2+} was measured using Fura-2 in transgenic cells expressing the red marker mCherry. In addition, elevations of the intracellular Ca^{2+} concentration was achieved by stimulating with blue light.

Calcium imaging enables measurement of activity of a large number of cells simultaneously. For instance, hundreds of neurons could be imaged and thus serve as a surrogate measure of the underlying electrical activity. In contrast to electrophysiology however, the time resolution is low.

4.5 ELECTROPHYSIOLOGY

In electrophysiology, electrical properties of living tissue are measured. It ranges from recording of single ion channels using patch-clamp under a microscope to diagnostics of epilepsy in patients using EEG. In the present thesis (**Paper II** and **III**), patch-clamp recordings were performed. In such, fine glass micropipettes containing physiological and defined solutions are attached to individual cells. Into the glass pipettes, metal wires are attached and connected to an amplifier. In whole-cell recording, an entire cell is attached to the pipette and currents through multiple ion channels are recorded simultaneously. By applying slight suction to the pipette, a high resistance seal around 10-100 GΩ is created. This "gigaseal" enables isolation of currents across the membrane with low noise.

4.6 OPTOGENETICS

The optogenetic approach is divided in two parts: light stimulation and preparing light sensitive cells. A light stimulation setup was engineered using blue LEDs mounted on a base attached to a heat sink. Light was focused with an optical lens (see **Figure 10**). Power was supplied via an electrical circuit including a relay controlled by a DAQ based system and custom-made computer software. Light sensitive cells were prepared by transducing HeLa cells with a lentiviral vector carrying the *OPN4* gene (melanopsin) tagged with mCherry. Next, transduced cells were sorted with flow-cytometry.

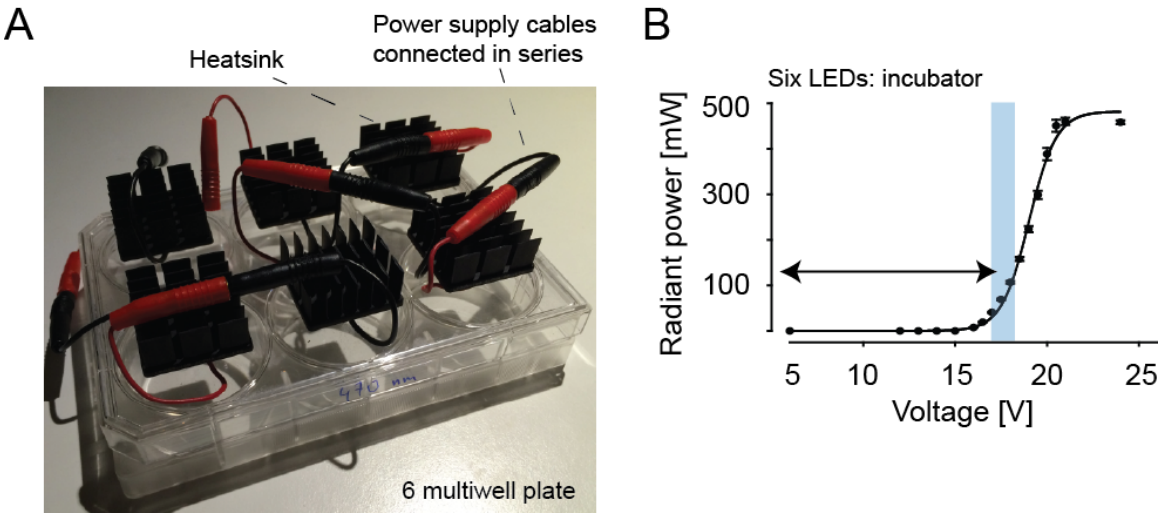

Figure 10 A) Optogenetics setup with six LEDs connected in series. B) Radiant power as a function of voltage.

4.7 TRANSCRIPTOMICS

RNA sequencing describes the technique of sequencing all RNA molecules present in a cell. By specifically targeting mRNA, this technique enables the identification and quantification of all transcribed genes. The set of all transcribed genes is called the transcriptome. By comparing the transcriptome of different groups of cells treated in different ways, one is able to infer differentially expressed genes. It all starts with collecting the cytoplasm of cells by lysis, reverse transcribing the mRNA to cDNA and finally to run PCR for a number of cycles for amplification. For bulk sequencing experiments, approximately 500 cells were used. Single cells were captured using C1 Single-Cell AutoPrep IFC microfluidic chip. The concentration and quality of the cDNA suspension was then measured using a fluorometric method (Qubit) and a miniature gel under microscope (Bioanalyzer). Next, a sequencing library was assembled with all individual samples multiplexed, by fragmentation and tagmentation. This was possible due to each sample having a unique sequence attached to all cDNA molecules. Also, the number of starting molecules of a certain species before any manipulation was known by the introduction of unique molecular identifiers [72]. Finally, the library was sent for massive parallel sequencing (Illumina HiSeq2000). Sequencing reads were filtered, aligned to the genome using Bowtie and finally annotated. Data files with counts and metadata were loaded into Matlab (Mathworks) and further analyzed with custom made scripts.

4.8 PHOSPHOPROTEOMICS

Protein phosphorylation is a common post-translational modification. Analogously to the transcriptome, the phosphoproteome is the set of all phosphorylated proteins. Just as for sequencing experiments, stimulated cells were first lysed. Thereafter, proteins were digested to peptides using trypsin, desalted and enriched for phosphopeptides using the Pierce TiO2 Phosphopeptide Enrichment and Clean-up Kit. Phosphopeptides were injected onto the nLC-MS/MS system (Ultimate^{TM} 3000 RSLCnano chromatography system and Q Exactive Plus Orbitrap mass spectrometer). The peptides were separated on a homemade C18 column. The effluent was electro sprayed into the mass spectrometer directly via the column. Proteins were identified by searching mgf files against the SwissProt database. Data files with counts were loaded into Matlab (Mathworks) and further analyzed with custom made scripts.

4.9 BIOINFORMATICS

Normalization of RNA sequencing counts for bulk experiments was performed using the lowess method. Further normalization was done to counts for cells expressing the empty vector and cells without light stimulation. Hypothesis testing for differential expression analysis was done using Student's t-test. Frequency dependent genes were defined as genes with fold change either above 2 or below 0.5 as well as q value less than 0.05. This resulted in approximately 100 genes. The hit genes were then characterized regarding gene ontology terms using the STRING database [73]. Next, possible upstream transcription factors controlling the expression of the hit genes were predicted using ChIP-X Enrichment Analysis [74] as part of the Expression2kinases software [75]. Next, a protein-protein interaction network around the transcription factors was predicted. Upstream kinases were subsequently identified by searching multiple databases for kinase-substrate data using Kinase Enrichment

Analysis [76]. Possible enrichment among the predicted signaling network was then analyzed by searching the KEGG database [77] with STRING.

Single cell RNA sequencing counts were filtered by removing data from cells with less than 2000 RNA molecules, resulting in 127 cells in total. The expression of hit genes from bulk sequencing data was analyzed and found to follow a Poisson distribution with added noise. Clustering was performed using principal component analysis with genes with the highest variance across all cells.

Phosphoproteomics data was analyzed in a similar way as bulk RNA sequencing data. Hypothesis testing for differential expression analysis was done using Student's t-test. Frequency dependent phosphoproteins were defines as those with fold change either above 2 or below 0.5 as well as q value less than 0.05. This resulted in approximately 100 phosphoproteins. Protein-protein interactions among the hits were analyzed using the STRING database [73].

4.10 NETWORK ANALYSIS

Connections in functional networks were found by applying cross-correlation, which quantifies the linear similarity between two waves as one of them is shifted in time [78]. In signal processing, waves are typically time series consisting of discrete sets of data points [X_t, $t \in T$], e.g., images acquired by time-lapse microscopy. The normalized version of the cross-correlation function, i.e., the cross-covariance, is commonly used for image-processing applications in which the brightness of the image is the quantitative measure. In MATLAB, the cross-covariance is implemented as *xcov* [79]:

$$c_{xy}(m) = \begin{cases} \sum_{n=0}^{N-|m|-1} (x(n+m) - \frac{1}{N}\sum_{i=0}^{N-1} x_i)\,(y_n^* - \frac{1}{N}\sum_{i=0}^{N-1} y_n^*) & if \quad m \geq 0 \\ c_{yx(-m)}^* & if \quad m < 0 \end{cases}$$

Here, m is the lag, N is the number of time points, n is the summation index, and x and y are the two time series. Correlations were deemed significant and considered to constitute a network link if the value was above a certain threshold. A scrambled data set $f_{scrambled}$ was created by shuffling the individual time series f to random starting points t. Thus, each original time series was divided into two parts at a random position and then put together again in the opposite order.

$$f_{scrambled}[1{:}N] = (f[t{:}N]\ f[1{:}t-1])$$

The total activity in the original data set and the scrambled data set was thereby conserved. The mean or the 99th percentile of the cross-covariance values of the scrambled data set can then be applied as the cut-off value.

There are several measures that can define a network. Connectivity is defined as the number of nodes with a correlation coefficient larger than the cut-off, divided by the total number of nodes. The edge density, also referred to as connectance [80], is defined as the number of edges divided by the maximum number of edges. The neighbors of a node are all the nodes connected to it in one step. The degree of a node is its number of neighbors; hence the degree

distribution $P(k)$ of a network is the distribution of nodes with a degree equal to k. $P(k)$ is obtained by counting the number of nodes $N(k)$ with $k = 1,2,3,\ldots$ connections and dividing by the total number of nodes.

In classical graph theory, models of networks occurring in nature are either regular or random. In a regular network, each node is connected to k other nodes [26]. In a random network, nodes are connected with links in a random fashion, resulting in a Poisson-shaped degree distribution around pN, where p is the probability and N is the total number of nodes. Small-world networks combine features of both regular and random networks, with high clustering as in regular networks but short internodal distances as in random networks [31]. The properties of small-world networks were assessed by calculating the mean clustering coefficient C and the mean shortest path length L of the network using the MatlabBGL library [81]. Hence, a small-world network was characterized by the following relations:

$$\sigma = \frac{C}{C_{rand}} \gg 1 \quad and \quad \lambda = \frac{L}{L_{rand}} \approx 1$$

The clustering coefficient is the number of neighbors of a node that are also neighbors of each other divided by the total number of possible links between the neighbors. Thus, it reflects the number of groups in a network. The shortest path length is the minimum number of nodes that must be passed to travel from one node to another. The values of C and L are then compared with the corresponding values of C_{rand} and L_{rand} for a randomized version of the network. A network is defined as possessing small-world characteristics if the mean path length is as short as in the corresponding random network, whereas the mean clustering coefficient is higher. The Barabási–Albert model of preferential attachment states that a scale-free network can be generated by allowing a random network to grow according to preferential attachment [30]. If the degree distribution approximately follows a power law (a heavy-tailed function without any clear mean value or scale), the network is defined as scale-free.

$$P(k) \propto k^{-\gamma} \leftrightarrow \log\big(P(k)\big) \propto -\gamma \log\,(k)$$

Scale-free networks have some nodes with many neighbors that can act as hubs [30].

4.11 MATHEMATICAL MODELING

In order to gain deeper insight into the mechanism behind spontaneous activity in neural progenitors, a mathematical model was developed for **Paper III**. In the model, the Ca^{2+} concentration in the cytosol and ER as well as the membrane potential was modeled as a function of time using ordinary differential equations. Traditionally, cell membranes have been modeled as electronic circuits with the phospholipid bilayer as a capacitor, the ion channels as resistors and electrochemical gradients as batteries [82]. Using Ohm's law, we have.

$$I = \frac{V}{R} = gV$$

Here, I is current, V potential, R resistance and g conductance. This holds true for every ionic species, but with unique variables. The driving voltage for instance for potassium can be written as:

$$V_{tot} = V - V_K$$

Where, in this case, V_K is the reverse potential for potassium determined by the Nernst equation:

$$V_{Nernst} = \frac{RT}{zF} \ln \frac{[ion]_{out}}{[ion]_{in}}$$

Here, R is the gas constant, F Faraday's constant, T the temperature and z valence.

For a parallel plate capacitor (which can model the lipid bilayer cell membrane) separating the charge q and voltage potential V, the capacitance C is given by:

$$C = \frac{q}{V}$$

Taking the time derivative gives (for constant C):

$$I_{cap} = \frac{dq}{dt} = C\frac{dV}{dt} = I_{ion} + I_{app}$$

In total, we thus have according to Kirchhoff's law (implemented in equation 1):

$$C\frac{dV}{dt} = -\sum_i g_i(V - V_i) + I_{app}$$

To solve this differential equation, one needs to establish the dependence of g on V and t. In 1963, Hodgkin and Huxley, together with John Eccles, received the Nobel Prize for their work on the voltage dependence of ion conductances in the electrically excitable membrane of the squid giant axon. It is outside the scope of this thesis to give a comprehensive description of the mathematics behind voltage gating. However, it is based on channels having gates that regulate the conductance. There may be both activation and inactivation gates based on the following mechanism:

$$C \overset{k_+,k_-}{\longleftrightarrow} O$$

Here, C is the closed state and O is the open state with rate constants k_+ and k_-. In **Paper III**, the so-called Morris-Lecar model describes the excitability. This model only involves a fast activating Ca^{2+} channel (similar to L-type channel), a delayed rectified K^+ current as well as a passive leak. The activation m_∞ is dependent on voltage as seen in **Figure 11** and describes the fraction of open channels. As seen below, it is only dependent on the voltage V, but not time. The opening probability of the potassium channel on the other hand is dependent on both time and voltage.

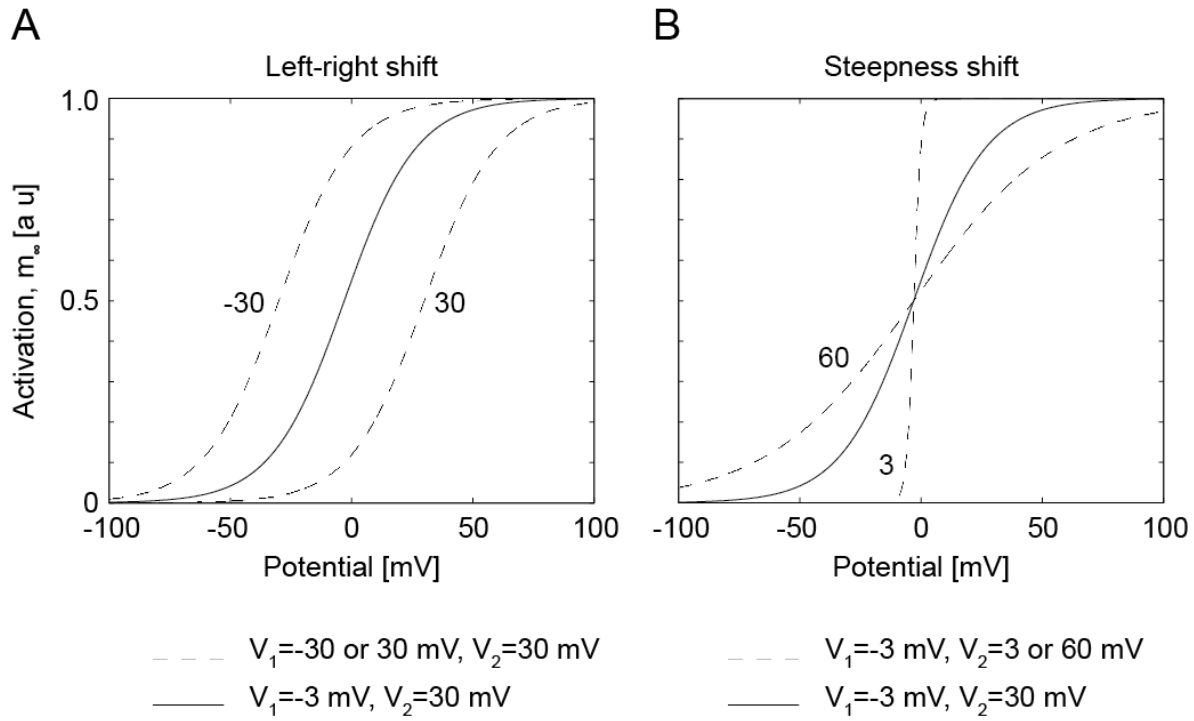

Figure 11 Voltage dependence of m_∞ as a function of A) V_1 and B) V_2.

Since the Morris-Lecar model only consists of two variables (potential V and fraction of open channels for the delayed rectifier K^+ channels w), the dynamics can be studies using phase plane analysis. This analysis will reveal the existence of a stable limit cycle upon current application (I_{app}), in other words oscillations in membrane potential as a function of time.

The Ca^{2+} concentration is modeled by describing the different fluxes of Ca^{2+} to and from the cytosol. Equations 3-5 include fluxes via both channels and pumps and are based on the conservation of Ca^{2+}.

The following equations constitute the mathematical model simulated in **Paper III**.
N different spherical cells with index $i, j \in \{1{:}\,N\}, i \neq j$ are interconnected.

1) $C_m \frac{dV_m^i}{dt} = I_{app} - g_K w\left(V_m^i - V_K\right) - g_{Ca} m_\infty \left(V_m^i - V_{Ca}\right) - \sum_{i=1}^{N} C(i,j) g_{gap}\left(V_m^i - V_m^j\right)$
2) $\frac{dw^i}{dt} = \varphi \frac{w_\infty - w^i}{\tau}$
3) $\frac{d[Ca^{2+}]_{cyt}^i}{dt} =$
$f_{cyt}[-\frac{\frac{3}{r^i}}{2F} g_{Ca} m_\infty \left(V_m^i - V_{Ca}\right) - J_{PMCA} + (v_{RYR} P_{RYR} + v_{leakER})\left([Ca^{2+}]_{ER}^i - [Ca^{2+}]_{cyt}^i\right) - J_{SERCA} + \sum_{i=1}^{N} (C(i,j) v_{gap} \left(\frac{r^j}{r^i}\right)^3 [Ca^{2+}]_{cyt}^j - [Ca^{2+}]_{cyt}^i)]$
4) $\frac{d[Ca^{2+}]_{tot}^i}{dt} = f_{cyt}[-\frac{\frac{3}{r^i}}{2F} g_{Ca} m_\infty \left(V_m^i - V_{Ca}\right) - J_{PMCA}]$
5) $[Ca^{2+}]_{ER}^i = \frac{[Ca^{2+}]_{tot}^i - [Ca^{2+}]_{cyt}^i}{\sigma}$

The connection between cells *i* and *j* is described by the matrix *C*.

$$C = \begin{pmatrix} C(1,1) & \cdots & C(1,N) \\ \vdots & \ddots & \vdots \\ C(N,1) & \cdots & C(N,N) \end{pmatrix}, \text{where } C(i,j) = \begin{cases} 1 \leftrightarrow i,j\ connected \\ 0 \leftrightarrow \neg\, i,j\ connected \end{cases}$$

The plasma membrane potential oscillator is described by the Morris-Lecar model [83].

$$m_\infty = 0.5[1 + \tanh(\frac{V_m^i - V_1}{V_2})]$$

$$w_\infty = 0.5[1 + \tanh(\frac{V_m^i - V_3}{V_4})]$$

$$\tau = \frac{1}{\cosh(\frac{V_m^i - V_3}{2V_4})}$$

The Ca^{2+} transporters are described by Hill functions [83].

$$J_{PMCA/SERCA} = \frac{v_{max,PMCA/SERCA}[Ca^{2+}]_{cyt}^2}{K_{1/2,PMCA/SERCA}^2 + [Ca^{2+}]_{cyt}^2}$$

The RyR is modeled as follows by Keizer and Levine [84] using a quasi-steady-state approximation [83].

$$P_{RyR} = n_\infty \frac{1 + (\frac{[Ca^{2+}]_{cyt}^i}{K_b})^3}{1 + (\frac{K_a}{[Ca^{2+}]_{cyt}^i})^4 + (\frac{[Ca^{2+}]_{cyt}^i}{K_b})^3}$$

$$n_\infty = \frac{1 + (\frac{K_a}{[Ca^{2+}]_{cyt}^i})^4 + (\frac{[Ca^{2+}]_{cyt}^i}{K_b})^3}{1 + \frac{1}{K_c} + (\frac{K_a}{[Ca^{2+}]_{cyt}^i})^4 + (\frac{[Ca^{2+}]_{cyt}^i}{K_b})^3}$$

Parameters are described in **Table 2**.

Table 2 Parameters and values with references.

Abbreviation	Numerical value	Unit	Description	Reference
C_m	1	$\mu F/cm^2$	Membrane capacitance per area	[83]
I_{app}	0	nA/cm^2	Applied current per area	Bifurcation parameter, starting with no applied current
g_K	20	$\mu S/cm^2$	K^+ channel conductance per area	[83]
V_K	-85	mV	K^+ channel reverse potential	[83]
g_{Ca}	20	$\mu S/cm^2$	Ca^{2+} channel conductance per area	Bifurcation parameter, starting from [83]
V_{Ca}	120	mV	Ca^{2+} channel reverse potential	[83]
g_{gap}	200	$\mu S/cm^2$	Gap junction conductance per area	Bifurcation parameter
v_{gap}	20	$1/s$	Gap junction Ca^{2+} permeability	Bifurcation parameter
f_{cyt}	0.003 decreased from 0.01 in [83])	1	Buffering factor	Chosen
φ	12	$1/s$	Rate constant of K^+ channel	[83]
r	10	μm	Radius of cells	Chosen
F	96500	C/mol	Faraday's constant	[83]
v_{RyR}	5	$1/s$	RyR permeability	[83]
$v_{leak,ER}$	0.2	$1/s$	ER leak permeability	[83]
σ	0.02	1	Ratio of effective ER and cytosol volumes	[83]
V_1	-3	mV	Ca^{2+} channel parameter,	[83]

			activation voltage	
V_2	30	*mV*	Ca^{2+} channel parameter, voltage width	[83]
V_3	-20	*mV*	K^+ channel parameter, activation voltage	[83]
V_4	30	*mV*	K^+ channel parameter, voltage width	[83]
$v_{max,PMCA}$	17 (increased from 5 in [83])	*μM/s*	Maximum transport rate	Chosen
$K_{1/2,\ PMCA}$	0.6	*μM*	Affinity for Ca^{2+}	[83]
$v_{max,\ SERCA}$	100	*μM/s*	Maximum transport rate	[83]
$K_{1/2,\ SERCA}$	0.2	*μM*	Affinity for Ca^{2+}	[83]
K_a	0.4	*μM*	RyR parameter	[83]
K_b	0.6	*μM*	RyR parameter	[83]
K_c	0.06 (decreased from 0.1 in [83])	*1*	RyR parameter	Chosen

4.12 MAGNETIC RESONANCE IMAGING

Magnetic resonance imaging is an imaging technique used in radiology. The method is based on the fact that certain atomic nuclei (usually hydrogen atoms in water or fat) can absorb and emit radio frequency energy when placed in a strong external magnetic field. The method was used in **Paper III** to study potential anatomical changes in the *Cacna1c* knockout mice. Brains of mice used for behavioral studies were perfused with a fixation agent in conjunction with a contrast agent using an active staining technique to increase the signal-to-noise-ratio and reduce the effective T1 in the MRI [85]. Scanning was done over night in a 9.4 T horizontal bore MRI-scanner. The spatial resolution is in the order of magnitude of 0.1 mm [86]. For example the volume of amygdala of a mouse brain is approximately 10 mm^3 [87].

4.13 MOUSE BEHAVIOUR

Mouse behavioral studies were performed in **Paper III** in order to find possible correlates of psychiatric symptoms in patients in the *Cacna1c* knockout mice. There are a wide variety of validated tests for mouse behavior related to for example anxiety, memory and aggression. Two of the most commonly used variants for anxiety-related behavior in mice are the open field test and elevated plus maze [88].

The open field test assesses novel environment exploration as well as locomotor activity. The environment is stressful to the mouse in two aspects: first because of physical separation from cage mates and second because of the unprotected, open environment by itself. Mice are acclimated to the test room and put in the center of the chamber. Next, a video camera records the movements for certain duration. Five minutes was used for assessing novel environment exploration, whereas longer time was used for habituation. Generally, mice will spend more time close to the walls than in the center. As an example, mice treated with anxiolytic drugs will spend more time in the center.

In the elevated plus maze, mice can spend time either in two open, unprotected arms or two enclosed, protected arms of the maze. The entire maze is elevated some distance from the floor. Mice are acclimated to the test room and put in the center of the maze. Next, a video camera records the movements for certain duration. Usually, mice tend to avoid the open arms.

5 RESULTS AND DISCUSSION

5.1 PAPER I: NETWORK ANALYSIS OF TIME-LAPSE MICROSCOPY RECORDINGS

Here, we developed methodology implemented in MATLAB to identify functional networks in groups of cells. By pairwise comparing time traces of for example Ca^{2+} dye intensity of multiple cells using cross-correlation, networks were constructed. The significance of correlation values was assessed by comparing them to the corresponding values of scrambled versions of the same traces. This way, the overall activity was considered although the exact timing of transients was neglected. Intercellular connections with correlation values above threshold were considered significant and considered as links in a functional network.

Next, the structure of the corresponding network was analyzed using methods from graph theory. For instance, the mean shortest path length and clustering coefficient could be calculated and used to classify the network. Networks were considered to have small-world properties if the mean shortest path length was as short as in corresponding random networks, whereas the mean clustering coefficient was higher. Scale free networks had no typical node degree (number of neighbors) as the degree distribution followed a power-law.

An obvious issue with this method is whether the functional networks identified really are based on underlying structural networks. In for example neural progenitors and atrial cardiomyocytes, cells are connected with gap junctions that enable intercellular communication. In one experiment, we recorded spontaneous Ca^{2+} activity in confluent cultures of HL-1 cells that had been exposed to a cut with a fine needle across the field of view. We could conclude that the physical division of cells into two populations was also found in the network analysis as two networks. Thus, the identified functional network is, at least partially, based on underlying physical connections.

5.2 PAPER II: NEURAL PROGENITORS ORGANIZE IN SMALL-WORLD NETWORKS TO PROMOTE CELL PROLIFERATION

Here, we identified spontaneous Ca^{2+} oscillations in neural progenitors derived from mouse embryonic stem cells that had been differentiating for ten days. Non-differentiated cells, however, exhibited much less activity. By employing the network identification and analysis tool described in **Paper I**, we found that the neural progenitors were organized in small-world networks with scale free properties. Also in whole E9.5 embryos, spontaneous oscillations were seen. In the next round of experiments, we sought to unravel important molecules involved in spontaneous activity. Cells *in vitro* were challenged with a multitude of drugs, including the purinergic receptor blocker suramin, sodium channel blocker tetrodotoxin and glutamate receptor inhibitors. None of these affected the spontaneous activity. Only removing extracellular Ca^{2+}, blocking VGCC with nickel or blocking gap junctions with octanol or flufenamic acid abolished the activity. shRNA mediated knockdown of Cx43 also decreased the activity. Whole cell patch clamp recording were performed on neural progenitors and showed that they also exhibit spontaneous firing that could be inhibited by nickel, cadmium and octanol. In order to validate the use of octanol as a gap junction blocker and to assess intercellular electrical conductance, multielectrode patch-clamp recordings were performed.

These showed that electrical current could be transmitted in-between cells and that this transmission could be blocked by octanol (and to some extent by the gap junction blockers flufenamic acid and 18α-glycyrrhetinic acid). Intercellular electrical transmission was then examined in E9.5 mouse embryonic brains and was also found to be responsive to octanol.

As previous studies have shown regulation of proliferation by Ca^{2+} oscillations in the developing cerebral cortex, we examined the effect both *in vitro* and *in vivo* in our hands. For neural progenitors derived from embryonic stem cells, blocking gap junctions with octanol or Cx43 shRNA reduced proliferation. Also nickel reduced cell division. However, the proliferation in embryonic stem cells was not affected by either octanol or nickel. In mouse E12.5 embryos, seven hours of treatment with octanol reduced proliferation in the dorsolateral cerebral cortex. Multiple days of octanol exposure (E12.5-E17.5) lead to smaller brain surface area as well as cortical layer formation. In conclusion, these *in vitro* and *in vivo* experiments indicate that neural progenitors wire up in functional networks that critically regulate proliferation.

Previous studies have reported spontaneous activity in neural progenitors and its role in regulating proliferation [8, 47, 48]. In the ventricular zone *in vivo*, Ca^{2+} activity has been shown to be dependent on gap junctions and ATP. Our data confirm the involvement of gap junctions, but at least *in vitro*, no involvement of purinergic receptors was found. Instead we provide evidence for involvement of VGCC in the plasma membrane. Nickel is claimed to be specific for T-type VGCC, whereas cadmium mainly block HVA channels [89]. Interestingly a few cells remained active upon gap junction inhibition, indicating the presence of trigger cells. **Paper III** will discuss this further.

Our data also reveal small-world networks with scale free properties. Thus, cells are not active at random, but are rather connected in a certain organization. One study reported that in the developing mouse hippocampus (P5-P7), neurons were organized in a scale free network with GABAergic cells as hubs [90]. Importantly, these hubs could control the activity of the entire network. The Barabasi and Albert mathematical model predicts that scale free networks are generated by adding new nodes to old nodes in a “rich get richer” fashion [30]. Thus, nodes with many neighbors have higher probability of being connected to new nodes. Small-world networks have been reported in for example newborn human brains [91] and cultured neurons [92]. The Watts and Strogatz mathematical model predicts that small-world networks arise as a few network links are rewired in a regular network [31]. Small-world networks provide a structure for efficient information flow and synchronized activity [26]. On the other hand, the existence of hubs in scale free networks, provide robustness to removal (cell death) of random nodes. We hypothesize that the scale free structure emerges as newborn cells are preferably connected to highly connected cells, since these may have more gap junction connections and more Ca^{2+} activity.

5.3 PAPER III: SPONTANEOUS ACTIVITY IN NEURAL PROGENITORS IS DRIVEN BY FUNCTIONAL PACEMAKERS EXPRESSING THE MOOD-DISORDER SUSCEPTIBILITY GENE *CACNA1C*

In this project we were interested in gaining deeper understanding of the mechanism behind spontaneous Ca^{2+} oscillations described in **Paper II** in general and to see the role of *Cacna1c*

in specific. For these purposes we developed a forebrain specific knockout mouse for *Cacna1c* using Emx1-Cre driver animals. In contrary to the habituation process of wild-type mice, the *Cacna1c* knockout mice increased their exploratory behavior in the open field test after five minutes. We could not detect any significant differences in the elevated plus maze, except for the knockout mice having more head dipping events. In whole brain MRI scanning experiments we detected significant changes in brain anatomy. In the knockout mice, there was an increase in striatum and periaqueductal grey (PAG) volume and decrease in hippocampus, neocortex and trigeminal tract. There was also a large, but non-significant increase in the volume of the mammillary bodies. By employing a multi-dimensional approach by merging all variables from MRI and behavioral experiments, we managed to cluster mice according to genotype using principal component analysis. Thus, forebrain specific deletion of *Cacna1c* led to signs of increased anxiety as well as changes in brain anatomy.

In preliminary experiments, we managed to record spontaneous Ca^{2+} activity during neural development in both knockout and wild type animals. There was a trend for knockout animals to have lower amplitudes of individual Ca^{2+} transients.

Next, we used neural progenitors derived from embryonic stem cells as a model of neural differentiation. Spontaneous activity arise around day six of differentiation as cells up regulate the expression of several ion channels, including *Cacna1c*, encoding the alpha 1c subunit of the L-type voltage gated calcium channel $Ca_V1.2$. Based on published (**Paper II**) and unpublished experimental data, we then developed a mathematical model in order to simulate the intracellular Ca^{2+} concentration and membrane potential. In the model, cells were interconnected with gap junctions permeable to both electrical current and Ca^{2+} to a varying degree. In addition, each cell had a time varying membrane potential as well as concentration of Ca^{2+} in the cytosol and ER. In the toolkit, cells also had RyR and SERCA that increases and decreases the cytosolic Ca^{2+} concentration, respectively. In a similar fashion, PMCA and VGCC control the influx via the plasma membrane. The membrane potential on the other hand is dependent on HVA VGCC and voltage dependent K^+ channels. We decided to use deterministic ordinary differential equations to model the Ca^{2+} dynamics. Thus, cells are considered to be zero dimensional objects or equivalently well stirred so that diffusion effects can be neglected. Furthermore, the modeled system is assumed to be noise-free and gap junctions are assumed to be passive elements with intercellular currents linearly increasing with voltage difference. By solving the equations using MATLAB, spontaneous oscillations in cytosolic Ca^{2+} and membrane potential appeared. Certain cells could act as functional pacemakers by having slightly higher conductance through VGCC. Next, we were able to investigate the parameter space even more by employing bifurcation analysis. In the model, spontaneous oscillations appear upon sufficient levels of gap junction and VGCC conductance. We investigated the oscillatory parameter space *in vitro* by measuring *Cacna1c* and *Cx43* expression with RT-qPCR as well as spontaneous Ca^{2+} activity as a function of differentiation time. Intriguingly, the shape of the developmental path *in vitro* is highly analogous to the *in silico* landscape.

One key element in the proposed model of spontaneous activity is the high similarity between pacemakers and non-pacemakers. The only difference in the model is the slightly higher conductance through VGCC. Based on this, we were able to estimate the number of

functional pacemakers *in vitro*, by using RT-qPCR data for *Cacna1c* expression in conjunction with bifurcation diagrams *in silico*. Using this, we found that approximately 20 % of all cells are pacemaker cells, which is almost completely coherent with the experimental value of ~19 %. In line with this, we next hypothesized that non-pacemaker cells could be converted to pacemaker cells and *vice versa*, by applying a positive or negative current, respectively. Combining Ca^{2+} imaging and patch clamp electrophysiology, we managed to confirm this. Cells with spontaneous oscillations in membrane potential were silenced upon injection of a small negative current (-5 pA), whereas silent cells were driven to activity by a small positive current (1 pA).

In conclusion, we have shown that forebrain specific deletion of *Cacna1c* leads to signs of increased anxiety as well as anatomical changes in brain regions known to be involved in anxiety. As an *in vitro* model of neural differentiation, neural progenitors up regulate *Cacna1c* as becoming spontaneously active. In a novel theoretical framework, spontaneous activity is driven by functional pacemaker cells expressing sufficient levels of *Cacna1c*, connected to other cells with gap junctions. In all, we hypothesize that changes in *Cacna1c* expression leads to erroneous spontaneous activity during development and increased susceptibility for later psychiatric disease.

5.4 PAPER IV: GENOMIC AND PROTEOMIC ANALYSES OF IMPACT OF CA^{2+} OSCILLATORY FREQUENCY

In this project we sought to develop methodology to control intracellular Ca^{2+} oscillations with optogenetics and to utilize it to find novel frequency decoders. We first developed a computer controlled light source and a polyclonal HeLa cell line expressing melanopsin as well as mCherry. Upon five seconds of blue light stimulation, melanopsin positive cells responded with a clear increase in cytosolic Ca^{2+} concentration. The increase was dependent on PLC as well as $InsP_3R$. Furthermore, the stimulation was gentle, as prolonged stimulation for 12 hours was not toxic.

In a first line of experiments, we assayed frequency dependence of the complete transcriptome by harvesting mRNA of stimulated cells for bulk and single cell RNA sequencing. We stimulated cells for either one hour or twelve hours with one Ca^{2+} transient every minute (≈ 15 mHz) or every second minute (≈ 8 mHz). After normalization to cells without stimulation as well as cells expressing only mCherry, differentially expressed genes were identified by comparing counts of cells stimulated with low frequency and high frequency. Comparing one hour of stimulation with twelve hours, there was only a minor overlap between the identified frequency dependent genes. Next, we tried to identify likely upstream proteins by searching databases for likely transcription factors and known protein-protein interactions. Upstream of these, we subsequently looked for kinases that may be responsible for relevant phosphorylations. Interestingly, there was a large overlap on kinase level when comparing one and twelve hours of stimulation. Using single cell RNA sequencing, we could conclude that hit genes from the bulk sequencing experiments were expressed as expected, following the Poisson distribution with added noise.

In analogous experiments, we employed phosphoproteomics to identify frequency dependent proteins and phosphoproteins. After light stimulation, proteins were harvested and enriched for phosphopeptides and analyzed with mass spectrometry. As for RNA sequencing data, we next identified differentially phosphorylated proteins and looked for likely upstream kinases. Interestingly, the predicted kinases partially overlapped with kinases inferred from RNA sequencing data. The following three kinases were inferred from both phosphoproteomics data and RNA sequencing data for one and twelve hours of stimulation: MAPK14, CSNK2A1 and GSK3B.

Among the genes and proteins identified as frequency dependent, several are related to NF-κB signaling. To more specifically study frequency decoding by NF-κB, we used a luciferase-based reporter assay. There was clear frequency dependence of the NF-κB transcription, with approximately seven times increase for stimulation with 15 mHz compared to no stimulation. As a next step, we used RT-qPCR to look for frequency dependence of genes regulated by NF-κB. Expression of the cytokines *TNF* and *IL8* was found to be frequency dependent as well as dependent on Ca^{2+} release via the $InsP_3R$ and NF-κB. By stimulating cells with a wider range of frequencies, we conclude that the frequency dependence of *TNF* and *IL8* is sigmoidal, with the maximum dynamic range around 10-20 mHz. To gain deeper understanding of the mechanism behind frequency decoding by *TNF* and *IL8*, we stimulated cells either with high frequency for half an hour or low frequency for one hour. Interestingly, the gene induction was significantly weaker for *TNF* with the lower frequency, whereas there was no difference for *IL8*. Thus, it seems as the frequency dependence is via the frequency itself and not total number of transients. In a similar fashion, we stimulated cells with either high frequency for one hour, or randomly, but with the same number of transients in total, for one hour. Intriguingly, also in this case the gene induction was significantly weaker with the random stimulation regime compared to the regular.

In conclusion, we short circuit the Ca^{2+} signaling system by directly controlling the cytosolic concentration using optogenetics and thereby bypass any kind of ligands binding to receptors as well as spontaneous activity. That way, we identify a network of frequency dependent genes and phosphoproteins and provide evidence for *bona fide* frequency dependence of *TNF* and *IL8*.

6 FUTURE PERSPECTIVES

The data presented above opens up for several important questions for future research.

- What is the function of functional networks *in vivo*? Do they tell us anything about adult neural circuits and function?

- How is proliferation controlled by Ca^{2+} oscillations?

- What is the physiological role of frequency decoding *in vivo* in general and in the developing brain in specific? Is the spontaneous activity optimized for downstream decoding?

- How does altered expression of *Cacna1c* lead to changes in brain anatomy and behaviour?

- Are other VGCC involved in spontaneous activity during development? What is the role of T-type channels?

7 GENERAL CONCLUSIONS

In general, the research described above deepens our understanding on Ca^{2+} oscillations and network activity. We have identified spontaneous activity in developing neurons and gained more insight into its underlying mechanism as well as physiological function. Developing neurons wire up in functional small-world networks with scale-free properties. These network formations are essential for normal development, as blocking them leads to decreased proliferation of neural progenitors in the ventricular zone. In addition, we have applied this knowledge in a model of mental disorder where the gene *Cacna1c* is deleted in the forebrain. These knockout mice have volumetric changes in several regions of the brain and show signs of increased anxiety. We have also developed a tool to control intracellular Ca^{2+} oscillations and thereby gained deeper understanding of the frequency dependence of signal transduction pathways.

8 ACKNOWLEDGEMENTS

A PhD is more than just an education and for me it certainly was. I first started working in the Uhlén group as Master thesis student from KTH in fall 2008, registered as PhD student in spring 2011 and now finally finish both my MD and PhD. All these years have been tremendously educative and would not have been possible without the support and help from all of you.

First of all, I would like to thank Professor **Per Uhlén** for first accepting me as Master thesis student and later on as PhD student. Your door has always been open for both professional and private conversations. I am grateful that you have accepted my sometimes far from straightforward career plans. Although you have let me completely free, you have always been there as a backup. I came as a somewhat naïve physicist and leaves as a father of two taking care of both my own experiments and patients. I am also grateful to **Sten Linnarsson**, who kindly accepted to take over as co-supervisor after **Cristian Ibarra** and **Ole Kiehn**. I am also grateful to my external mentor **Hugo Lagercrantz**.

Thank you **Arthur Konnerth** for taking your time to be my opponent, it's a true honor! To **Dinos Meletis**, **Anders Tengholm** and **Erik Fransén**, thank you for your expertise on my examination board. Thank you **Mitya** for being the chairman of my defense.

Thanks to all the previous and present members of MolNeuro. Thanks to **Patrik Ernfors**, **Ernest Arenas**, **Sten Linnarsson**, **Jens Hjerling-Leffler, Gonçalo Castelo-Branco** and **Ulrika Marklund**, for creating a great environment for research.

In the **Per Uhlen group**: **Ivar** (for friendship and good collaboration in the lab, good luck with medical school), **Staffan** (for nice discussion on philosophy and politics), **Dagmara** (I know you will become a great scientist and good luck with your wedding), **Paola** (for teaching me when I was new in the lab), **Seth** (for company in Palo Alto), **Shigeaki** (for your hard work and Japanese sweets), **Nobu** (for your dedicated work with a clinical approach), **Songbai** (for your endless work on GIT), **Marie** (for helping me when I was new in the lab), **Simone** (for your rock'n'roll science), **Cristian** (for your pharmacological perspective), **Manuel** (for your help with lentiviruses and for being a very nice guy), **Lauri** (for asking me tough questions on science and for being a good friend with *sisu*), **Teresa** (for helping me with 2-photon imaging), **Ibrahim** (I hope to see you more in research), **Nicolas** (for your French attitude and for hanging out in New York), **Göran** and **Connla** (for helping out with microscopy).

In the other groups: **Spiros** (for all table tennis matches and early lunches), **Enrique** (for sharing office and listening to my bad jokes), **Daniel** (for good company during lunch time and your hard work), **Shanzheng** (for your kindness and collaboration), **Alca** (for being so positive), **Carmen** (for always being nice and interested), **Boris** (for your Italian spirit), **Martin**, **Changgeng**, **Lili** (for always being interested and chatting about children and work), **Hind**, **Alessandro**, **Mortiz**, **Dauhua**, **Jana** (for being a great organizer), **Dongoh**, **Hermany** (for discussions on career plans and psychiatry), **Carolina** (for your nice attitude), **Kasra** (good luck with the rest of your PhD), **Nathan**, **Ana**, **Shaimaa** (for your friendship), **Amit** (for your sense of humor and help with sequencing), **Pawel**, **Una** (for being a power woman),

Kasper, **Anna J**, **Hannah** (good luck with your little gift), **Lars**, **Gioele**, **David**, **Ana**, **Mandy**, **Sueli**, **Viktoria**, and **Fatima**. **Johnny, Ahmad** and **Alessandra**, you make the lab running. Also, thanks to all my numerous collaborators (among others): **Michael**, **Roman**, **Tibor**, **Eric**, **David**, **Shuijie, Susanne**, **Min** and **Jesper**.

To my friends from KTH: **Erik**, **Fredrik**, **Matthias** and **Daniel**. I hope we will meet in the future and see where an education in engineering physics may lead. And to **Martin**, I am glad I got to know you. Keep up the coffee engineering work!

To my friends from medical school. **Arash** (my best Iranian friend).

Göran, **Jonatan** och **Mattis**, my best friends, you have all followed me during all these years, in despair and happiness. För fortsatt vänskap! Last but not least, I would like to thank my family. Tack **mamma** och **pappa** för ert stöd genom hela uppväxten och skoltiden och därefter och tack **Marie**, **Björn** och **Martin** med respektive för ert tålamod med mig. **Farmor** och **farfar**, ni har alltid varit så snälla och visat intresse för min forskning. **Bull**, **Mona** och **Linnéa**, ni har verkligen fått mig att känna mig välkommen i er familj.

Anna, utan dig vore jag mindre än halv. Du och jag för alltid. Vi har tillsammans skapat våra fina barn. Nu är äntligen åren med låga inkomster och dubbla arbetsuppgifter över. Jag hoppas och tror att det har varit värt det. **Fredrika** och **Siri**, det finns inget som gör mig gladare än att se er tillsammans. Forsätt att följa er nyfikenhet och världen kommer att ligga öppen för er.

9 REFERENCES

1. Berridge, M.J., *Cell Signalling Pathways*, in *Cell Signalling Biology*. 2014.
2. Berridge, M.J., M.D. Bootman, and H.L. Roderick, *Calcium signalling: dynamics, homeostasis and remodelling.* Nat Rev Mol Cell Biol, 2003. **4**(7): p. 517-29.
3. Clapham, D.E., *Calcium signaling.* Cell, 2007. **131**(6): p. 1047-58.
4. Uhlen, P., et al., *Calcium signaling in neocortical development.* Dev Neurobiol, 2015. **75**(4): p. 360-8.
5. Berridge, M.J., P. Lipp, and M.D. Bootman, *The versatility and universality of calcium signalling.* Nat Rev Mol Cell Biol, 2000. **1**(1): p. 11-21.
6. Berridge, M.J., M.D. Bootman, and P. Lipp, *Calcium--a life and death signal.* Nature, 1998. **395**(6703): p. 645-8.
7. Zhang, S., et al., *Inositol 1,4,5-trisphosphate receptor subtype-specific regulation of calcium oscillations.* Neurochem Res, 2011. **36**(7): p. 1175-85.
8. Weissman, T.A., et al., *Calcium waves propagate through radial glial cells and modulate proliferation in the developing neocortex.* Neuron, 2004. **43**(5): p. 647-61.
9. Berridge, M.J., *The AM and FM of calcium signalling.* Nature, 1997. **386**(6627): p. 759-60.
10. Mikoshiba, K., *IP3 receptor/Ca2+ channel: from discovery to new signaling concepts.* J Neurochem, 2007. **102**(5): p. 1426-46.
11. Bezprozvanny, I., J. Watras, and B.E. Ehrlich, *Bell-shaped calcium-response curves of Ins(1,4,5)P3- and calcium-gated channels from endoplasmic reticulum of cerebellum.* Nature, 1991. **351**(6329): p. 751-4.
12. Putney, J.W., *Capacitative calcium entry: from concept to molecules.* Immunol Rev, 2009. **231**(1): p. 10-22.
13. Catterall, W.A., et al., *International Union of Pharmacology. XLVIII. Nomenclature and structure-function relationships of voltage-gated calcium channels.* Pharmacol Rev, 2005. **57**(4): p. 411-25.
14. Berridge, M.J., *Calcium signalling and cell proliferation.* Bioessays, 1995. **17**(6): p. 491-500.
15. Kapur, N., G.A. Mignery, and K. Banach, *Cell cycle-dependent calcium oscillations in mouse embryonic stem cells.* Am J Physiol Cell Physiol, 2007. **292**(4): p. C1510-8.
16. See, V., et al., *Calcium-dependent regulation of the cell cycle via a novel MAPK--NF-kappaB pathway in Swiss 3T3 cells.* J Cell Biol, 2004. **166**(5): p. 661-72.
17. Salazar, C., A.Z. Politi, and T. Hofer, *Decoding of calcium oscillations by phosphorylation cycles: analytic results.* Biophys J, 2008. **94**(4): p. 1203-15.
18. Smedler, E. and P. Uhlen, *Frequency decoding of calcium oscillations.* Biochim Biophys Acta, 2014. **1840**(3): p. 964-9.
19. Berridge, M.J., *Remodelling Ca2+ signalling systems and cardiac hypertrophy.* Biochem Soc Trans, 2006. **34**(Pt 2): p. 228-31.

20. Kupzig, S., S.A. Walker, and P.J. Cullen, *The frequencies of calcium oscillations are optimized for efficient calcium-mediated activation of Ras and the ERK/MAPK cascade.* Proc Natl Acad Sci U S A, 2005. **102**(21): p. 7577-82.

21. De Koninck, P. and H. Schulman, *Sensitivity of CaM kinase II to the frequency of Ca2+ oscillations.* Science, 1998. **279**(5348): p. 227-30.

22. Dolmetsch, R.E., K. Xu, and R.S. Lewis, *Calcium oscillations increase the efficiency and specificity of gene expression.* Nature, 1998. **392**(6679): p. 933-6.

23. Boyden, E.S., et al., *Millisecond-timescale, genetically targeted optical control of neural activity.* Nat Neurosci, 2005. **8**(9): p. 1263-8.

24. Gradinaru, V., K.R. Thompson, and K. Deisseroth, *eNpHR: a Natronomonas halorhodopsin enhanced for optogenetic applications.* Brain Cell Biol, 2008. **36**(1-4): p. 129-39.

25. Qiu, X., et al., *Induction of photosensitivity by heterologous expression of melanopsin.* Nature, 2005. **433**(7027): p. 745-9.

26. Feldt, S., P. Bonifazi, and R. Cossart, *Dissecting functional connectivity of neuronal microcircuits: experimental and theoretical insights.* Trends Neurosci, 2011. **34**(5): p. 225-36.

27. Jeong, H., et al., *Lethality and centrality in protein networks.* Nature, 2001. **411**(6833): p. 41-2.

28. Malmersjo, S., et al., *Neural progenitors organize in small-world networks to promote cell proliferation.* Proc Natl Acad Sci U S A, 2013. **110**(16): p. E1524-32.

29. Sporns, O., G. Tononi, and R. Kotter, *The human connectome: A structural description of the human brain.* PLoS Comput Biol, 2005. **1**(4): p. e42.

30. Barabasi, A.L. and R. Albert, *Emergence of scaling in random networks.* Science, 1999. **286**(5439): p. 509-12.

31. Watts, D.J. and S.H. Strogatz, *Collective dynamics of 'small-world' networks.* Nature, 1998. **393**(6684): p. 440-2.

32. Pfenniger, A., A. Wohlwend, and B.R. Kwak, *Mutations in connexin genes and disease.* Eur J Clin Invest, 2011. **41**(1): p. 103-16.

33. Wiencken-Barger, A.E., et al., *A role for Connexin43 during neurodevelopment.* Glia, 2007. **55**(7): p. 675-86.

34. Hu, X. and G. Dahl, *Exchange of conductance and gating properties between gap junction hemichannels.* FEBS Lett, 1999. **451**(2): p. 113-7.

35. Elias, L.A. and A.R. Kriegstein, *Gap junctions: multifaceted regulators of embryonic cortical development.* Trends Neurosci, 2008. **31**(5): p. 243-50.

36. Mallo, M., D.M. Wellik, and J. Deschamps, *Hox genes and regional patterning of the vertebrate body plan.* Dev Biol, 2010. **344**(1): p. 7-15.

37. Gulisano, M., et al., *Emx1 and Emx2 show different patterns of expression during proliferation and differentiation of the developing cerebral cortex in the mouse.* Eur J Neurosci, 1996. **8**(5): p. 1037-50.

38. Gorski, J.A., et al., *Cortical excitatory neurons and glia, but not GABAergic neurons, are produced in the Emx1-expressing lineage.* J Neurosci, 2002. **22**(15): p. 6309-14.

39. Spitzer, N.C., *Electrical activity in early neuronal development.* Nature, 2006. **444**(7120): p. 707-12.

40. Meister, M., et al., *Synchronous Bursts of Action-Potentials in Ganglion-Cells of the Developing Mammalian Retina.* Science, 1991. **252**(5008): p. 939-943.

41. Gonzalez-Islas, C. and P. Wenner, *Spontaneous network activity in the embryonic spinal cord regulates AMPAergic and GABAergic synaptic strength.* Neuron, 2006. **49**(4): p. 563-575.

42. Tritsch, N.X., et al., *The origin of spontaneous activity in the developing auditory system.* Nature, 2007. **450**(7166): p. 50-+.

43. Garaschuk, O., E. Hanse, and A. Konnerth, *Developmental profile and synaptic origin of early network oscillations in the CA1 region of rat neonatal hippocampus.* Journal of Physiology-London, 1998. **507**(1): p. 219-236.

44. Watt, A.J., et al., *Traveling waves in developing cerebellar cortex mediated by asymmetrical Purkinje cell connectivity.* Nature Neuroscience, 2009. **12**(4): p. 463-473.

45. Ben-Ari, Y., et al., *GABAA, NMDA and AMPA receptors: a developmentally regulated 'menage a trois'.* Trends Neurosci, 1997. **20**(11): p. 523-9.

46. Blankenship, A.G. and M.B. Feller, *Mechanisms underlying spontaneous patterned activity in developing neural circuits.* Nature Reviews Neuroscience, 2010. **11**(1): p. 18-29.

47. Liu, X., et al., *Gap junctions/hemichannels modulate interkinetic nuclear migration in the forebrain precursors.* J Neurosci, 2010. **30**(12): p. 4197-209.

48. Liu, X., et al., *The role of ATP signaling in the migration of intermediate neuronal progenitors to the neocortical subventricular zone.* Proc Natl Acad Sci U S A, 2008. **105**(33): p. 11802-7.

49. Owens, D.F. and A.R. Kriegstein, *Patterns of intracellular calcium fluctuation in precursor cells of the neocortical ventricular zone.* J Neurosci, 1998. **18**(14): p. 5374-88.

50. Yuste, R., et al., *Neuronal domains in developing neocortex: mechanisms of coactivation.* Neuron, 1995. **14**(1): p. 7-17.

51. Weissman, T.A., et al., *Calcium waves propagate through radial glial cells and modulate proliferation in the developing neocortex.* Neuron, 2004. **43**(5): p. 647-661.

52. Dalmau, J., et al., *Paraneoplastic anti-N-methyl-D-aspartate receptor encephalitis associated with ovarian teratoma.* Ann Neurol, 2007. **61**(1): p. 25-36.

53. Belmaker, R.H., *Bipolar disorder.* N Engl J Med, 2004. **351**(5): p. 476-86.

54. Merikangas, K.R., et al., *Prevalence and correlates of bipolar spectrum disorder in the world mental health survey initiative.* Arch Gen Psychiatry, 2011. **68**(3): p. 241-51.

55. Edvardsen, J., et al., *Heritability of bipolar spectrum disorders. Unity or heterogeneity?* J Affect Disord, 2008. **106**(3): p. 229-40.

56. Saha, S., et al., *A systematic review of the prevalence of schizophrenia.* PLoS Med, 2005. **2**(5): p. e141.

57. Gejman, P.V., A.R. Sanders, and J. Duan, *The role of genetics in the etiology of schizophrenia.* Psychiatr Clin North Am, 2010. **33**(1): p. 35-66.

58. Cardno, A.G. and M.J. Owen, *Genetic relationships between schizophrenia, bipolar disorder, and schizoaffective disorder.* Schizophr Bull, 2014. **40**(3): p. 504-15.

59. Schizophrenia Psychiatric Genome-Wide Association Study, C., *Genome-wide association study identifies five new schizophrenia loci.* Nat Genet, 2011. **43**(10): p. 969-76.

60. Psychiatric, G.C.B.D.W.G., *Large-scale genome-wide association analysis of bipolar disorder identifies a new susceptibility locus near ODZ4.* Nat Genet, 2011. **43**(10): p. 977-83.

61. Sullivan, P.F., M.J. Daly, and M. O'Donovan, *Genetic architectures of psychiatric disorders: the emerging picture and its implications.* Nat Rev Genet, 2012. **13**(8): p. 537-51.

62. Hell, J.W., et al., *Identification and differential subcellular localization of the neuronal class C and class D L-type calcium channel alpha 1 subunits.* J Cell Biol, 1993. **123**(4): p. 949-62.

63. Ertel, E.A., et al., *Nomenclature of voltage-gated calcium channels.* Neuron, 2000. **25**(3): p. 533-5.

64. Dolmetsch, R.E., et al., *Signaling to the nucleus by an L-type calcium channel-calmodulin complex through the MAP kinase pathway.* Science, 2001. **294**(5541): p. 333-9.

65. Graef, I.A., et al., *L-type calcium channels and GSK-3 regulate the activity of NF-ATc4 in hippocampal neurons.* Nature, 1999. **401**(6754): p. 703-8.

66. Lipscombe, D., T.D. Helton, and W. Xu, *L-type calcium channels: the low down.* J Neurophysiol, 2004. **92**(5): p. 2633-41.

67. Ying, Q.L., et al., *Conversion of embryonic stem cells into neuroectodermal precursors in adherent monoculture.* Nat Biotechnol, 2003. **21**(2): p. 183-6.

68. Conesa, A., et al., *A survey of best practices for RNA-seq data analysis.* Genome Biol, 2016. **17**: p. 13.

69. Reiner, A., D. Yekutieli, and Y. Benjamini, *Identifying differentially expressed genes using false discovery rate controlling procedures.* Bioinformatics, 2003. **19**(3): p. 368-75.

70. Grynkiewicz, G., M. Poenie, and R.Y. Tsien, *A new generation of Ca2+ indicators with greatly improved fluorescence properties.* J Biol Chem, 1985. **260**(6): p. 3440-50.

71. Li, S., et al., *The 1p36 Tumor Suppressor KIF 1Bbeta Is Required for Calcineurin Activation, Controlling Mitochondrial Fission and Apoptosis.* Dev Cell, 2016. **36**(2): p. 164-78.

72. Islam, S., et al., *Quantitative single-cell RNA-seq with unique molecular identifiers.* Nat Methods, 2014. **11**(2): p. 163-6.

73. Szklarczyk, D., et al., *STRING v10: protein-protein interaction networks, integrated over the tree of life.* Nucleic Acids Res, 2015. **43**(Database issue): p. D447-52.

74. Lachmann, A., et al., *ChEA: transcription factor regulation inferred from integrating genome-wide ChIP-X experiments.* Bioinformatics, 2010. **26**(19): p. 2438-44.

75. Chen, E.Y., et al., *Expression2Kinases: mRNA profiling linked to multiple upstream regulatory layers.* Bioinformatics, 2012. **28**(1): p. 105-11.

76. Lachmann, A. and A. Ma'ayan, *KEA: kinase enrichment analysis.* Bioinformatics, 2009. **25**(5): p. 684-6.

77. Kanehisa, M. and S. Goto, *KEGG: kyoto encyclopedia of genes and genomes.* Nucleic Acids Res, 2000. **28**(1): p. 27-30.

78. Peter J. Brockwell, R.A.D., *Time Series: Theory and Methods*. 2 ed. Springer Series in Statistics. 1998, New York: Springer. 600.

79. The MathWorks, I., *xcov* 2009, The MathWorks, Inc. .

80. Newman, M., *Networks: An Introduction*. 1 ed. 2010: Oxford University Press. 720.

81. Gleich, D., *MatlabBGL*. 2006, The MathWorks, Inc. .

82. Hodgkin, A.L. and A.F. Huxley, *A quantitative description of membrane current and its application to conduction and excitation in nerve.* J Physiol, 1952. **117**(4): p. 500-44.

83. Fall CP, M.E., Wagner JM and Tyson JJ, *Computational Cell Biology*. Interdisciplinary Applied Mathematics. Vol. 20. 2002: Springer. 468.

84. Keizer, J. and L. Levine, *Ryanodine receptor adaptation and Ca2+(-)induced Ca2+ release-dependent Ca2+ oscillations.* Biophysical Journal, 1996. **71**(6): p. 3477-87.

85. Johnson, G.A., et al., *A multidimensional magnetic resonance histology atlas of the Wistar rat brain.* Neuroimage, 2012. **62**(3): p. 1848-56.

86. Budde, J., et al., *Ultra-high resolution imaging of the human brain using acquisition-weighted imaging at 9.4T.* Neuroimage, 2014. **86**: p. 592-8.

87. Badea, A., A.A. Ali-Sharief, and G.A. Johnson, *Morphometric analysis of the C57BL/6J mouse brain.* Neuroimage, 2007. **37**(3): p. 683-93.

88. Bailey, K.R. and J.N. Crawley, *Anxiety-Related Behaviors in Mice*, in *Methods of Behavior Analysis in Neuroscience*, J.J. Buccafusco, Editor. 2009: Boca Raton (FL).

89. Simms, B.A. and G.W. Zamponi, *Neuronal voltage-gated calcium channels: structure, function, and dysfunction.* Neuron, 2014. **82**(1): p. 24-45.

90. Bonifazi, P., et al., *GABAergic hub neurons orchestrate synchrony in developing hippocampal networks.* Science, 2009. **326**(5958): p. 1419-24.

91. Fransson, P., et al., *The functional architecture of the infant brain as revealed by resting-state fMRI.* Cereb Cortex, 2011. **21**(1): p. 145-54.

92. Downes, J.H., et al., *Emergence of a small-world functional network in cultured neurons.* PLoS Comput Biol, 2012. **8**(5): p. e1002522.